The Abdus Salam
International Centre for Theoretical Physics

United Nations
Educational, Scientific
and Cultural Organization

International Atomic
Energy Agency

World Year of PHYSICS 2005

H4.SMR/1642-3

"IAG-IASPEI Joint Capacity Building Workshop on Deformation Measurements and Understanding Natural Hazards in Developing Countries"

17 - 23 January 2005

Important Earthquakes at the Contact Alps-Dinarides Junction

P. Suhadolc

Department of Earth Sciences
University of Trieste

Strada Costiera 11, 34014 Trieste, Italy - Tel. +39 040 2240 111; Fax +39 040 224 163 - sci_info@ictp.it, www.ictp.it

Important Earthquakes at the Alps-Dinarides Junction

Peter Suhadolc

Department of Earth Sciences
University of Trieste

IAG-IASPEI Joint Capacity Building Workshop - ICTP 2004

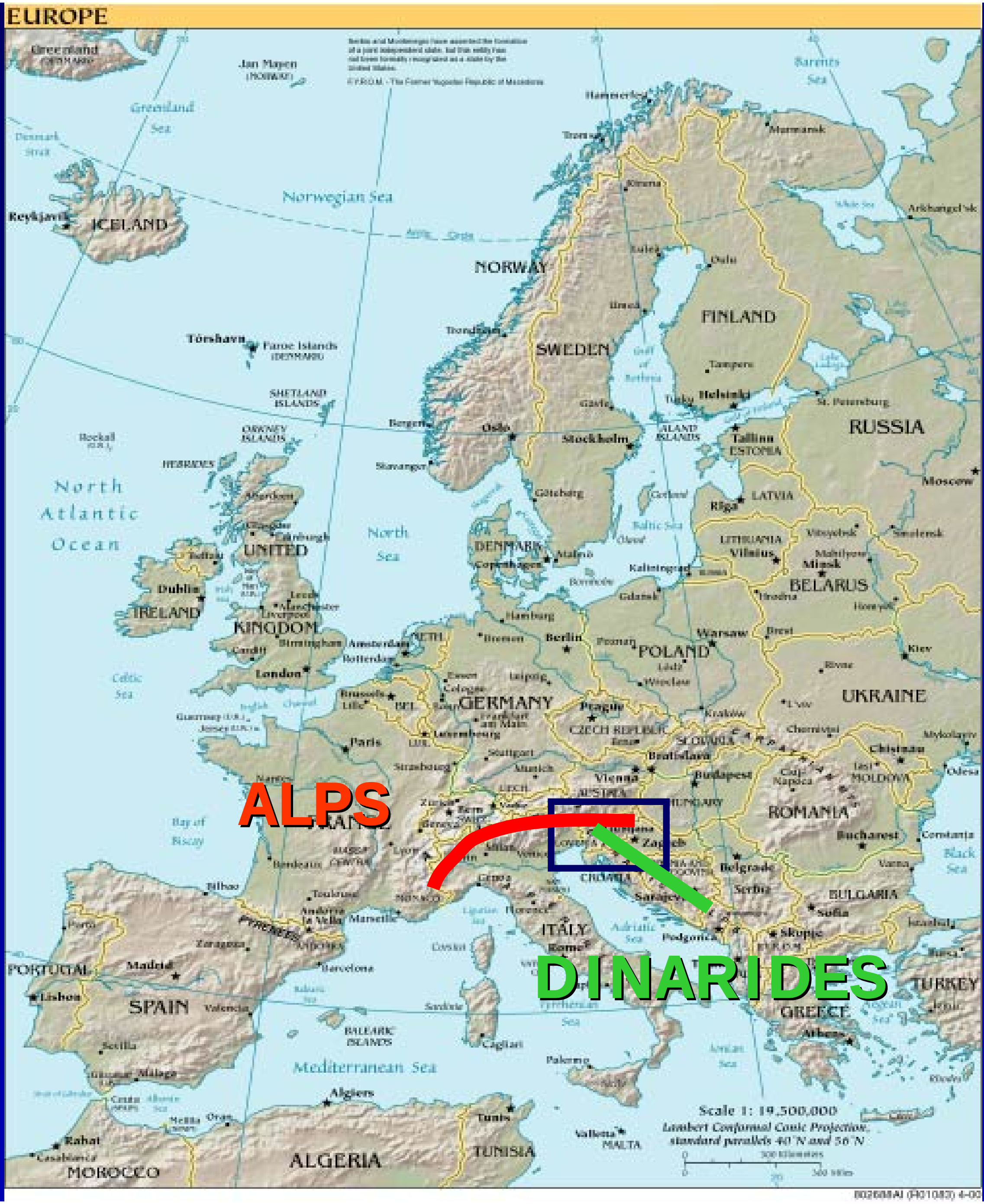
EUROPE
ALPS
DINARIDES
NORWAY
SWEDEN
FINLAND
RUSSIA
ICELAND
UNITED KINGDOM
IRELAND
GERMANY
POLAND
UKRAINE
BELARUS
ROMANIA
ITALY
SPAIN
PORTUGAL
ALGERIA
MOROCCO
TUNISIA
GREECE
TURKEY
North Atlantic Ocean
North Sea
Norwegian Sea
Mediterranean Sea
Scale 1: 19,500,000

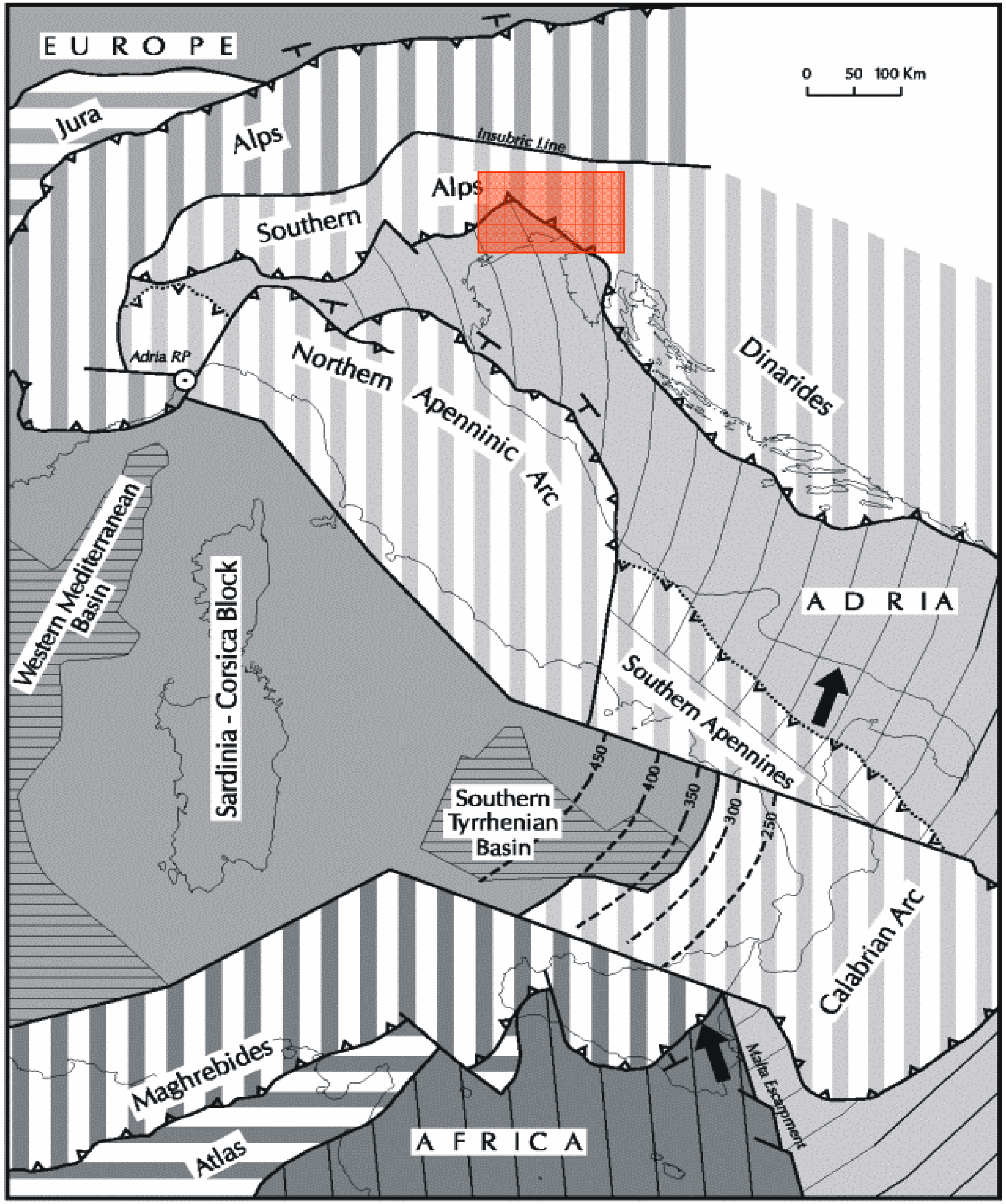

Geodynamic Framework

Historical seismicity

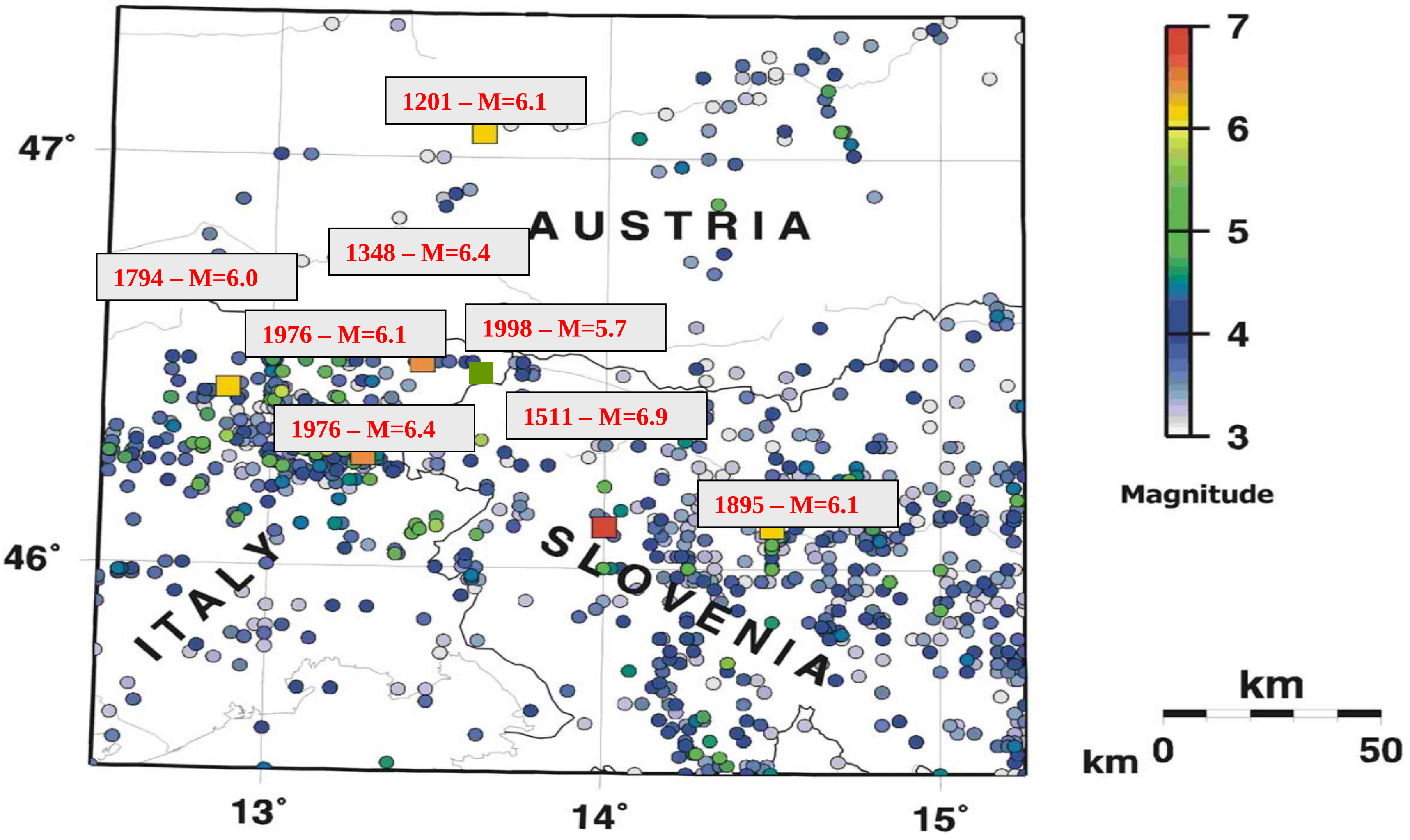

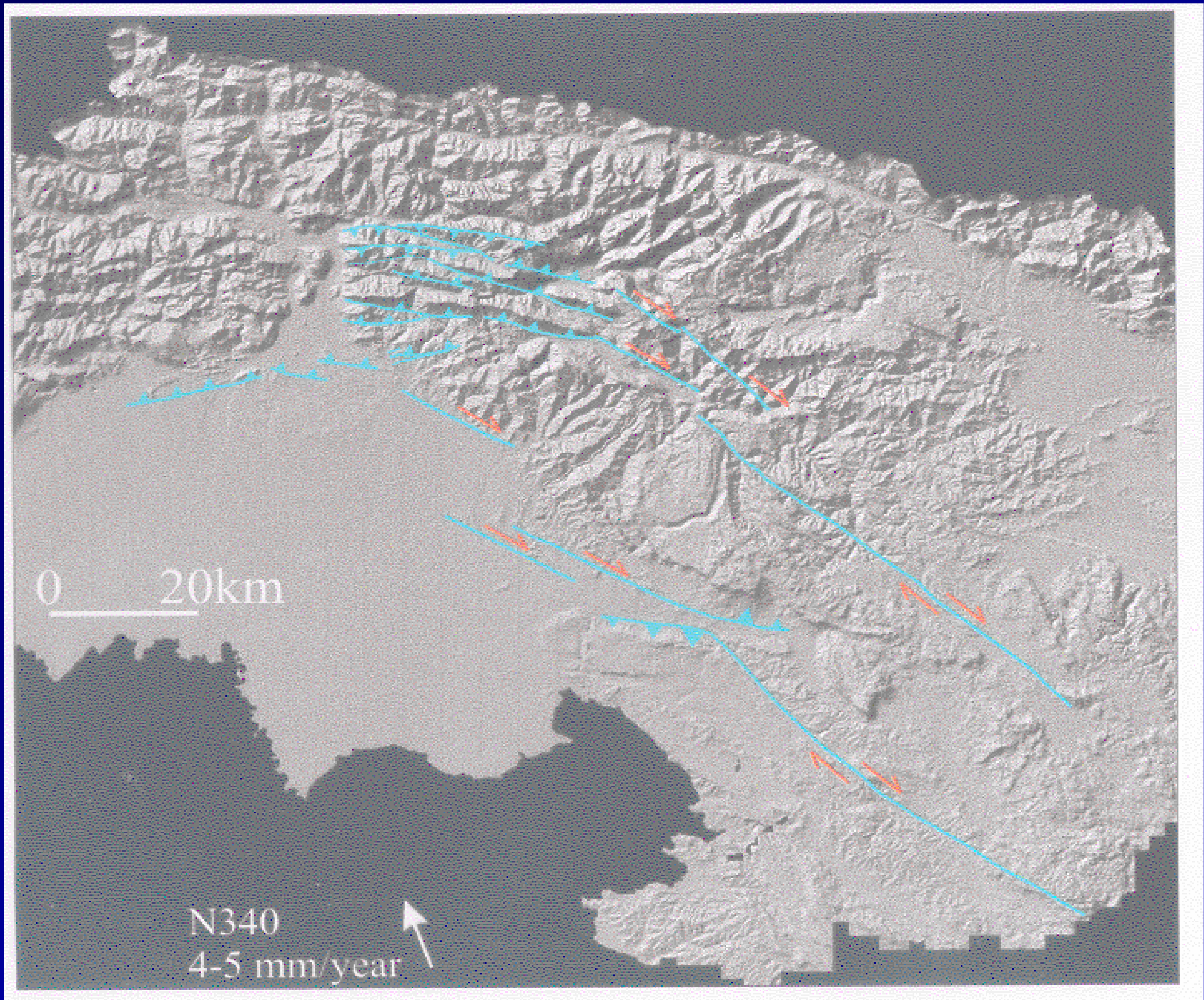

Active faults in NE Italy and W Slovenia

Aoudia(1999)

- # The 1511 Earthquake

Constraints on the Location and Mechanism of the 1511 Western-Slovenia Earthquake from Active Tectonics and Modeling of Macroseismic Data

The March 26th, 1511 Earthquake

Is the largest event occurred at the Alps-Dinarides Junction

I_{max} **10** (Boschi et al., 2000; Cecic, 2000)

Its aftershock sequence lasted until 1516
(Ambraseys, 1976; Ribaric, 1979)

It killed about 12,000 people
(Ambraseys, 1976; Ribaric, 1979)

No attempt so far to identify a possible causative structure

Single shock or two shocks?

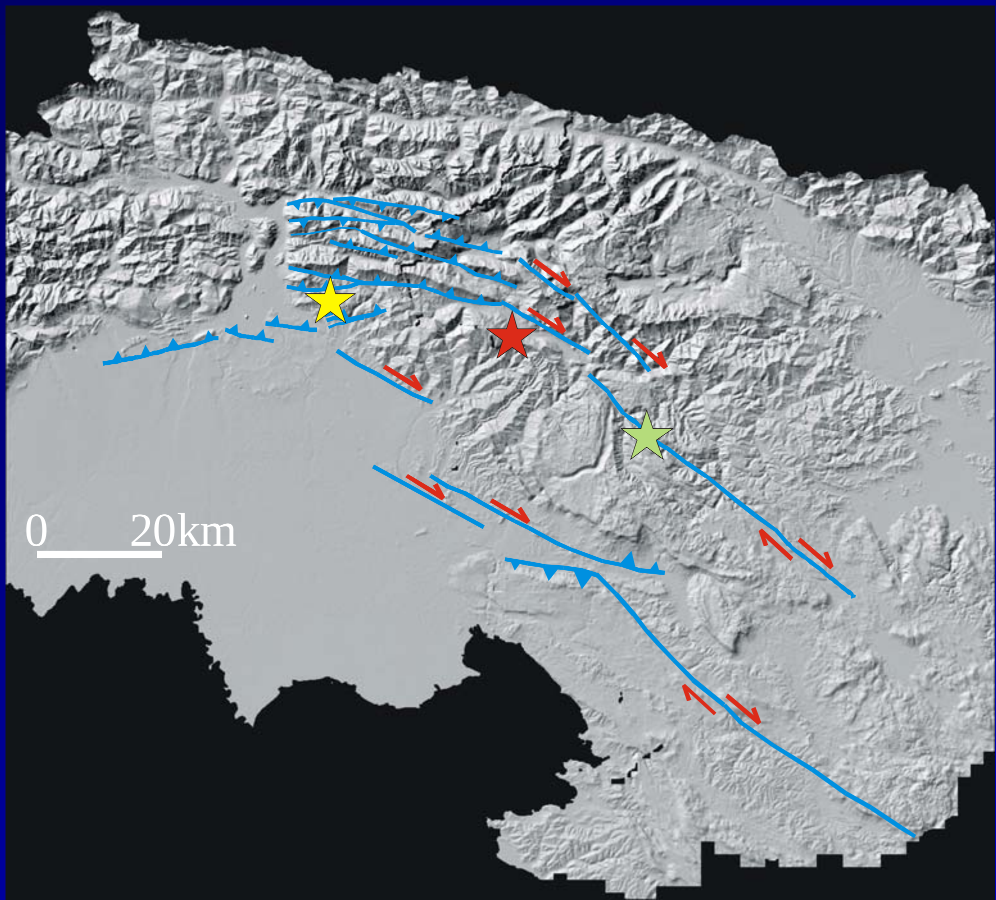

Ambraseys, 1976

h 20:15 M 6.4
ϕ 13.6 λ 46.2

Ribaric, 1979

h 15:00 M 6.9
ϕ 14.0 λ 46.1

h 20-20:30 M 7.0-7.2
ϕ 13.4 λ 46.2

Boschi et al., 2000

h 14:40 M 6.9
ϕ 13.43 λ 46.20

Intensity Database and Macroseismic Field

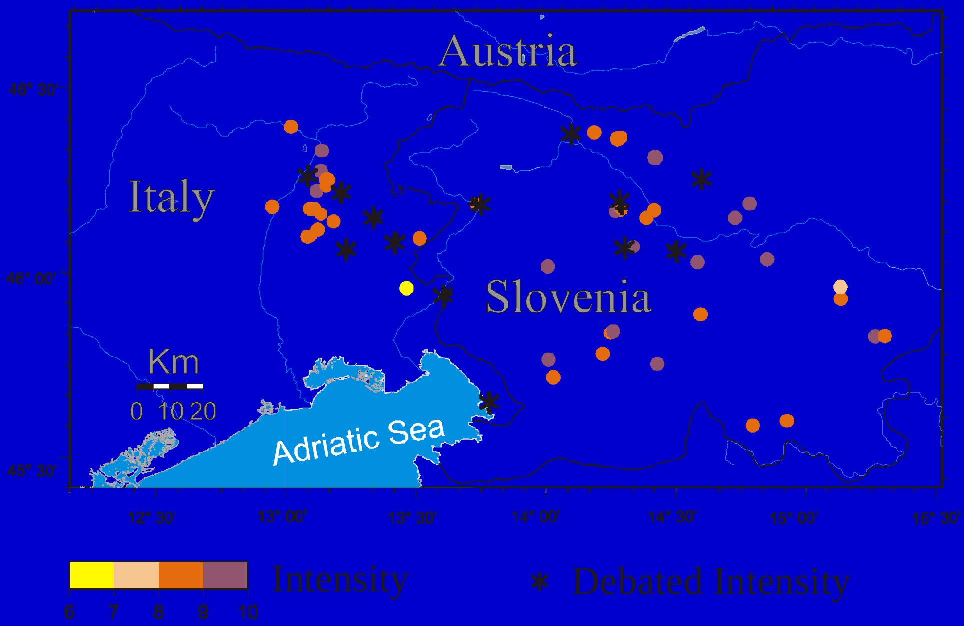

DOM4.1 (Monachesi et al., 1997)
CFT3 (Boschi et al., 2000)
Cecic, 2000

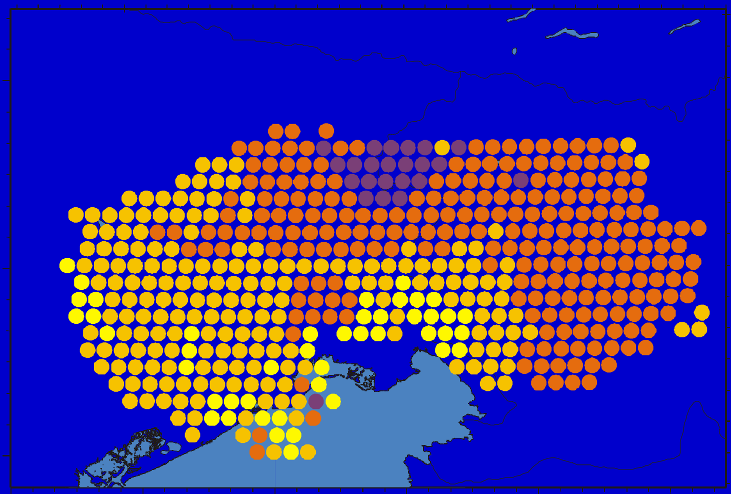

Macroseismic Field
Computed by Polinomial Filtering
(Kronrod, 2001)

Two Possible Scenarios

Two-shocks Scenario

↓

Cumulative Effect of a Mainshock and a Strong Aftershock

Single-Shock Scenario

↓

A Single Event

Method

Active Tectonics

Identification of possible causative structures

Synthetic Seismograms (1 Hz)

Modal Summation for Extended Sources

(Panza, 1985; Panza and Suhadolc, 1987; Florsch at al., 1991, Sarao’ et al., 1998; Panza et al., 2001)

+

Different Nucleation Points,
Constant Rupture Propagation Models
Uniform Seismic Moment Distribution

Maximum Horizontal Velocities

Misfit between Observed and Computed Intensities

The maximum horizontal velocities are converted to intensities by means of an empirical relation

Misfit between Observed and Computed Intensities: The Modified Databases

Maximized Observed Intensity Database

e.g. VII/VIII ⟶ VIII

Intensity	DMAX(cm)	VMAX(cm/s)	DGA(g)
V	0.1-0.5	0.5-1.0	0.005-0.01
VI	0.5-1.0	1.0-2.0	0.01-0.02
VII	1.0-2.0	2.0-4.0	0.02-0.04
VIII	2.0-3.5	4.0-8.0	0.04-0.08
IX	3.5-7.0	8.0-15.0	0.08-0.15
X	7.0-15.0	15.0-30.0	0.15-0.30
XI	15.0-30.0	30.0-60.0	0.30-0.60

(Panza et al., 2001)

Minimized Observed Intensity Database

e.g. VII/VIII ⟶ VII

Misfit between Observed and Computed Intensities: The Parameters

$$d_i = \left| I_{OBS} - I_{CALC} \right|$$

$$\bar{d} = \frac{\sum d_i}{N}$$ → **Rounded to Integer Value**

$$d_{tot} = \sum d_i$$

Two-Shocks Scenario: Input Fault Models

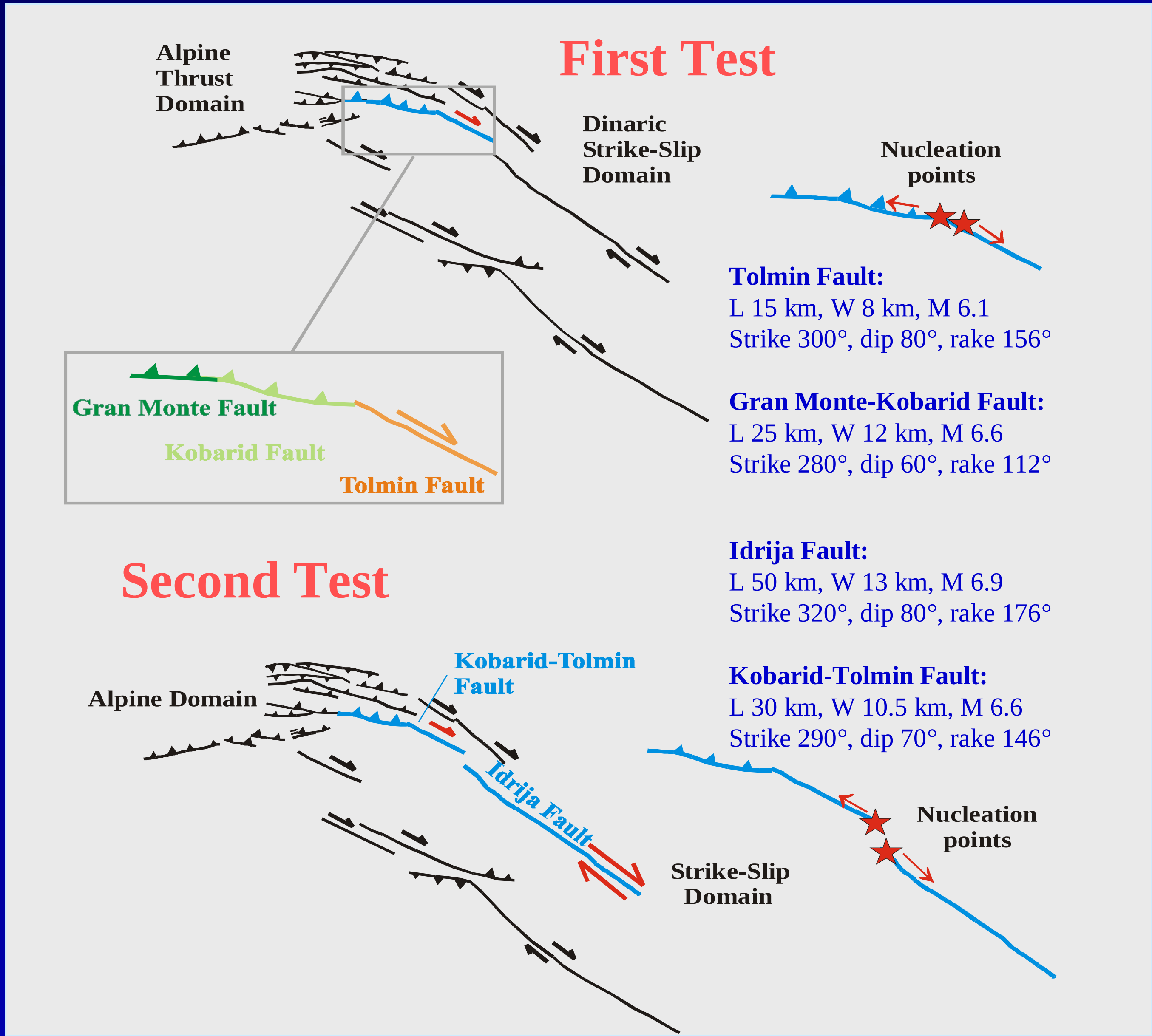

Two-Shocks Scenario: Results 1st Test

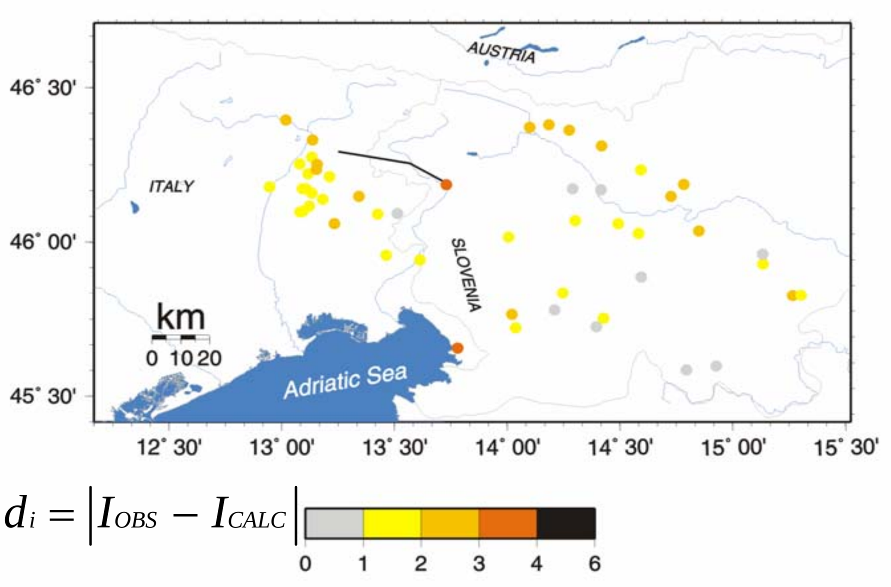

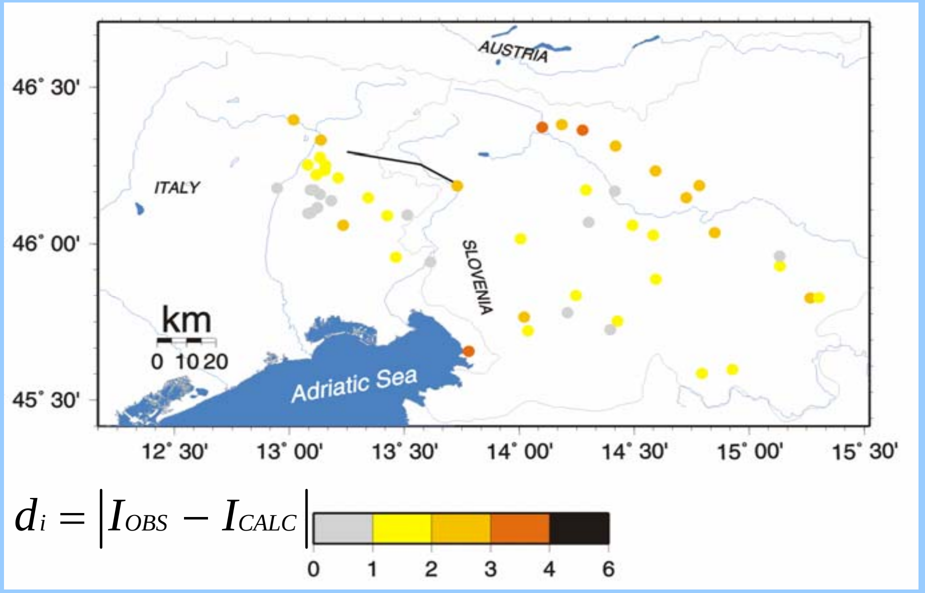

Minimized Observed Intensity Database:

$\overline{d} = 1$ $\qquad d_{tot} = 61$

$d_i = 0 \longrightarrow$ 9 sites

Maximized Observed Intensity Database:

$\overline{d} = 1$ $\qquad d_{tot} = 54$

$d_i = 0 \longrightarrow$ 15 sites

Two-Shocks Scenario: Results 2nd Test

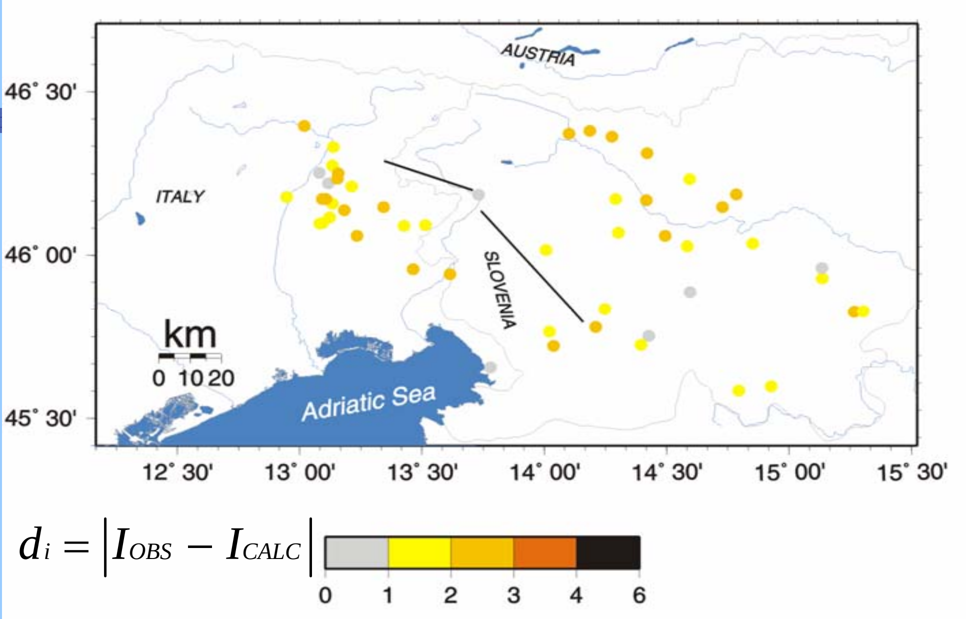

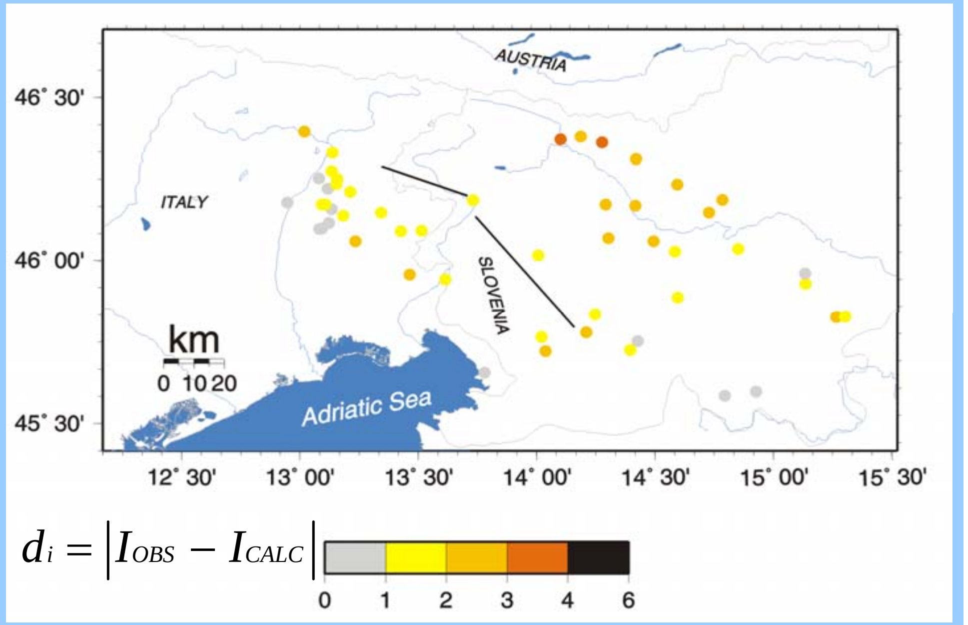

Minimized Observed Intensity Database:

$\bar{d} = 1$ $d_{tot} = 65$

$d_i = 0$ ⟶ 7 sites

Maximized Observed Intensity Database:

$\bar{d} = 1$ $d_{tot} = 58$

$d_i = 0$ ⟶ 12 sites

Single Shock Scenario

Maximum Horizontal Acceleration Field (Point source 0.1Hz) vs Observed Macroseismic Field, for 2 Source Mechanisms

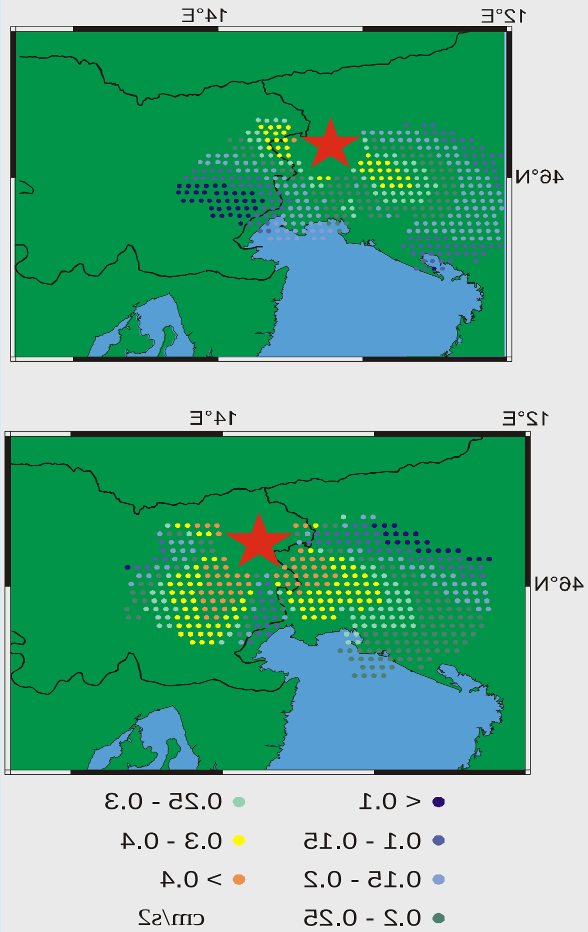

Thrust

θ 288°
δ 29°
λ 112°

Strike-slip

θ 320°
δ 80°
λ 180°

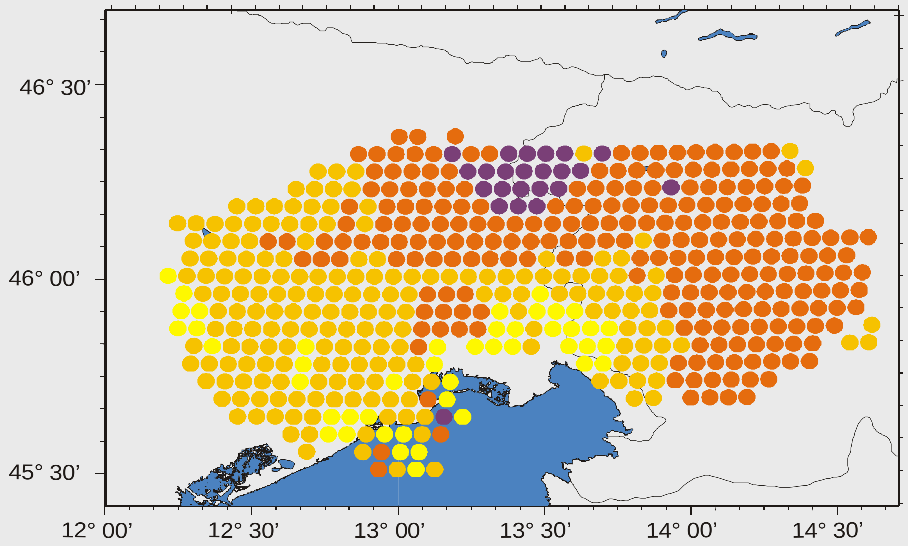

Macroseismic Field

(Kronrod, 2001)

The Idrija Strike-slip System

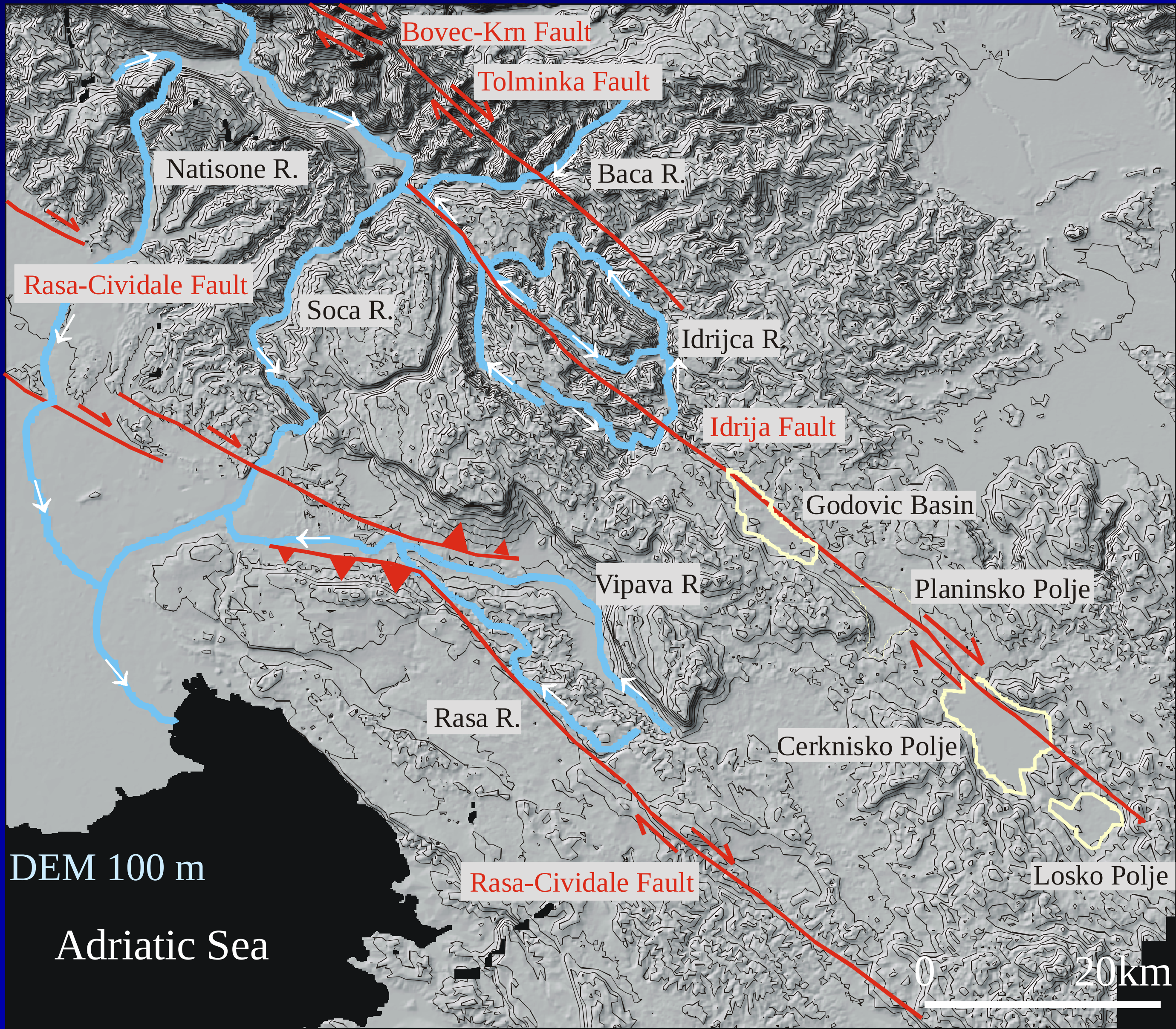

Single Shock Scenario: Input Fault Models

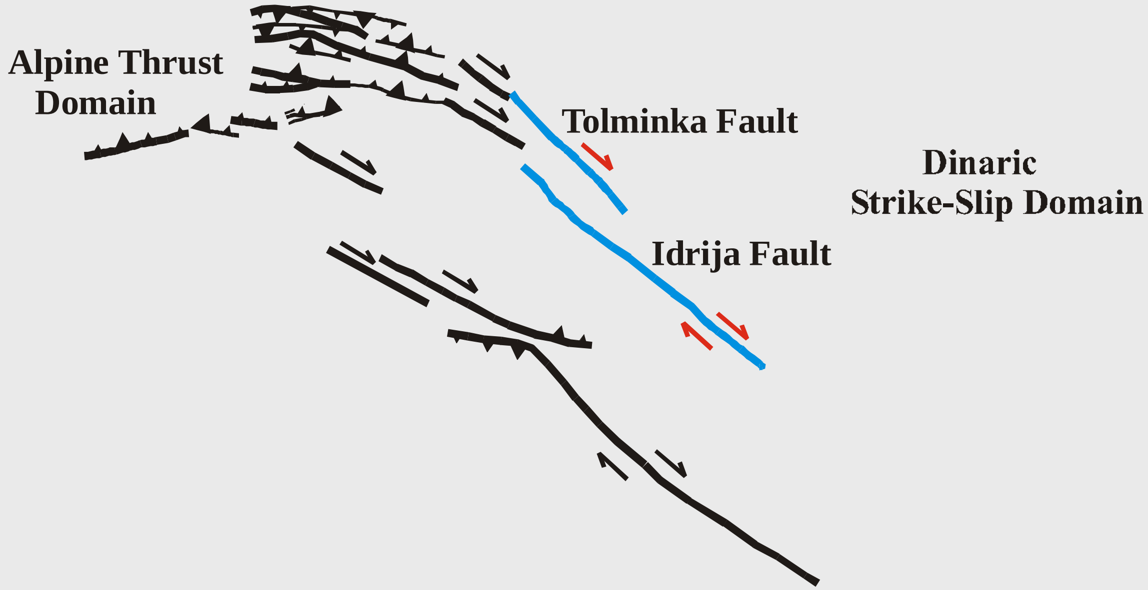

First Test

Nucleation points

Tolminka Fault

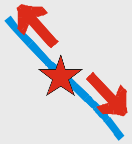

Tolminka Fault:
L 30 km, W 10 km, M 6.6
Strike 320°, dip 80°, rake 176°

Second Test

Nucleation points

Idrija Fault

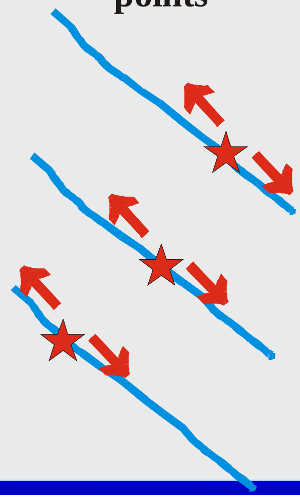

Idrija Fault:
L 50 km, W 13 km, M 6.9
Strike 320°, dip 80°, rake 180°

Single Shock Scenario: Results 1st Test

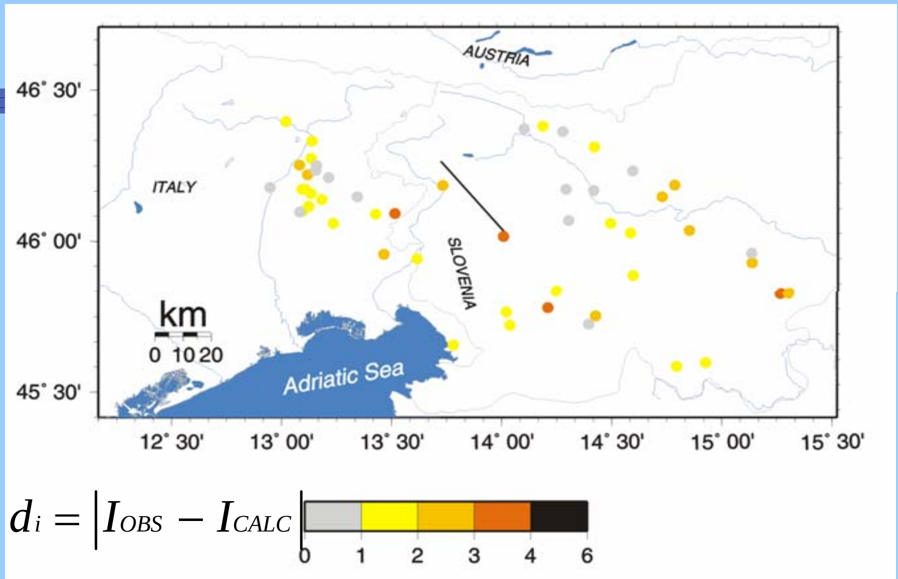

Minimized Observed Intensity Database:

$\overline{d} = 1$ $d_{tot} = 55$

$d_i = 0 \longrightarrow$ 14 sites

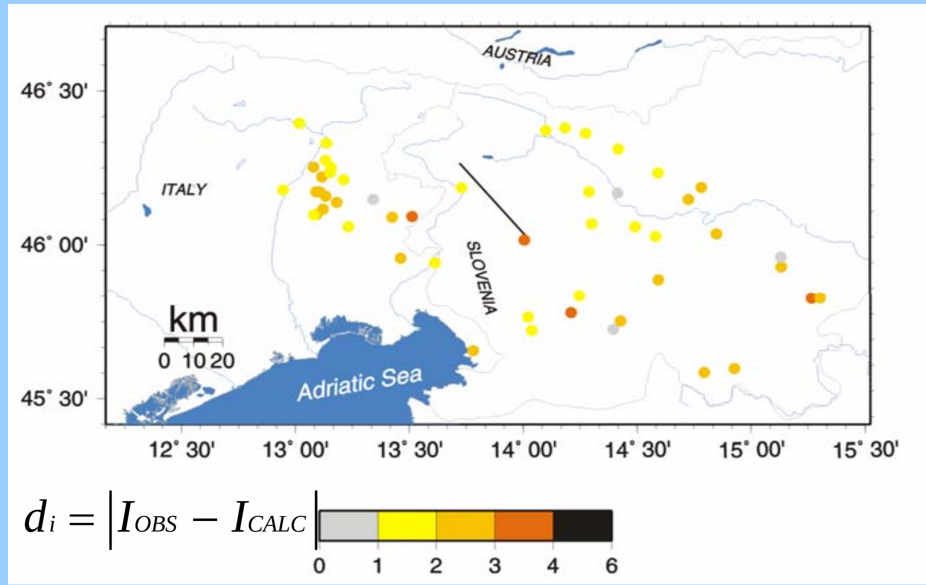

Maximized Observed Intensity Database:

$\overline{d} = 1$ $d_{tot} = 75$

$d_i = 0 \longrightarrow$ 4 sites

Single Shock Scenario: Results 2nd Test

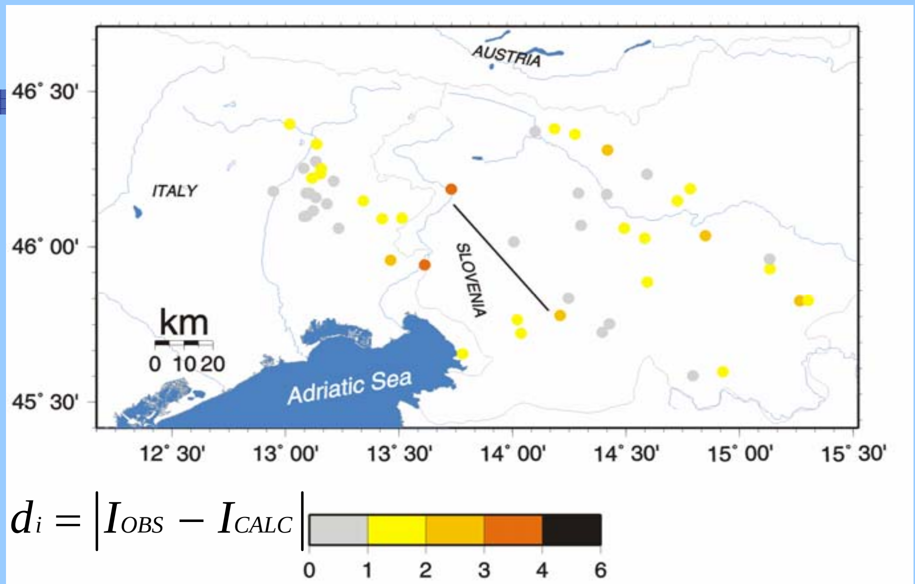

Minimized Observed Intensity Database:

$\overline{d} = 1$ $\quad d_{tot} = 37$

$d_i = 0 \longrightarrow$ 23 sites

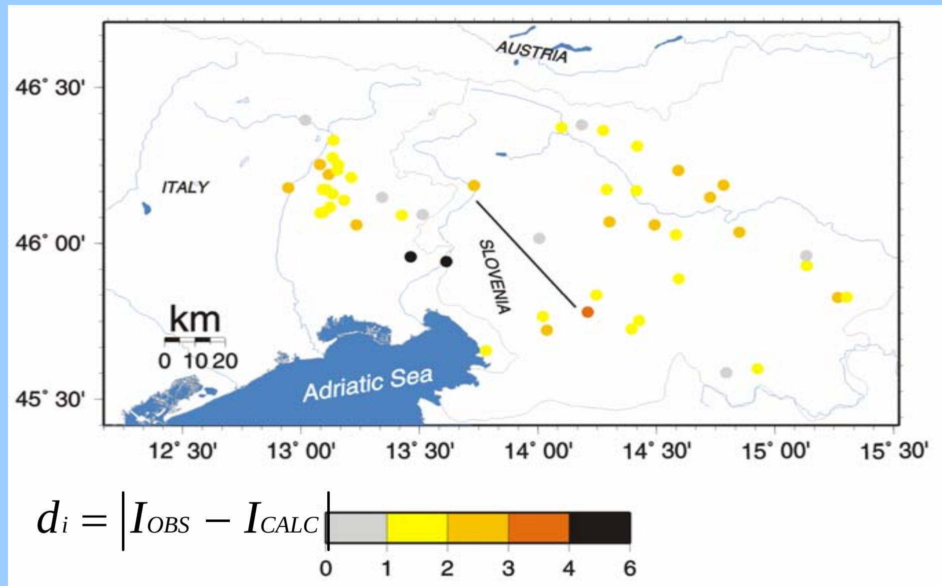

Maximized Observed Intensity Database:

$\overline{d} = 1$ $\quad d_{tot} = 49$

$d_i = 0 \longrightarrow$ 13 sites

Discussion

Misfit between Observed and Computed Intensities

		$\bar{d}$	d_{tot}	$d = 0$
2-Shocks Scenario	Min.	1	61	9
First Test	Max.	1	54	15
2-Shocks Scenario	Min.	1	65	7
Second Test	Max.	1	58	12
1-Shock Scenario	Min.	1	55	14
First Test	Max.	1	75	4
1-Shock Scenario	Min.	1	37	23
Second Test	Max.	1	49	13

Conclusions

- The best misfit between theoretical results and observed data is obtained for a **single shock** with a **strike-slip** mechanism.
- The possible causative structure is the **Idrija** right-lateral strike-slip fault.

Forward modeling of the Friuli 1976 (NE Italy) event

Active deformation and recent seismicity

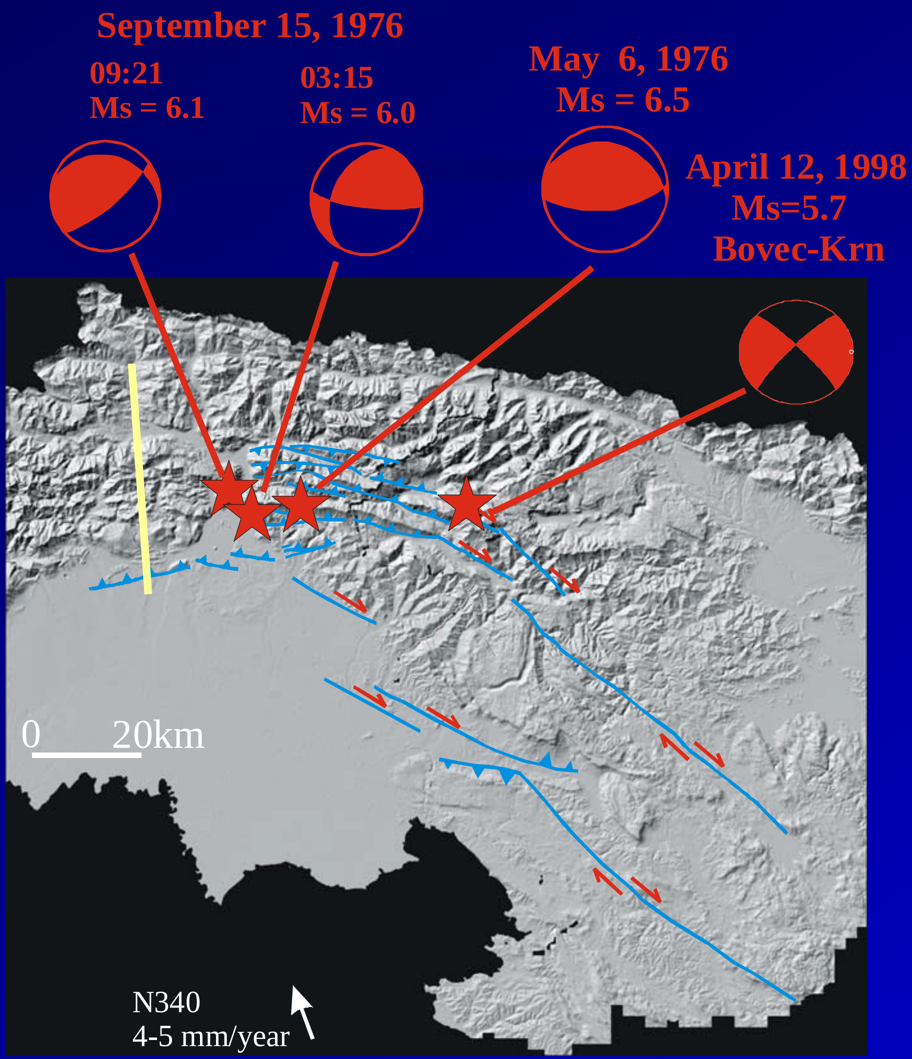

Microseismicity 1977-1987 (Renner, 1995)

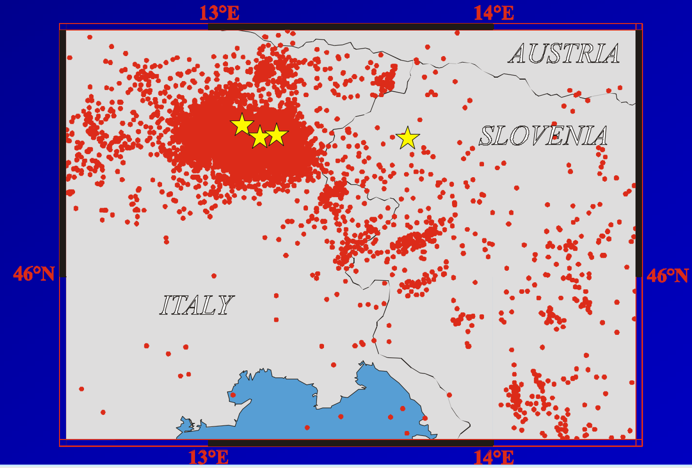

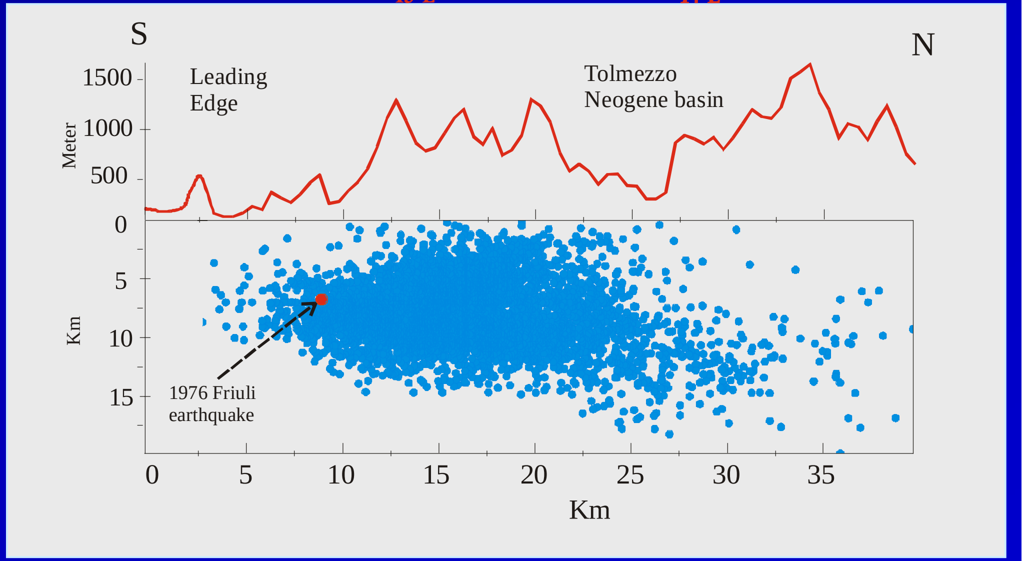

The 1976 Friuli thrust fault and related earthquake sequence

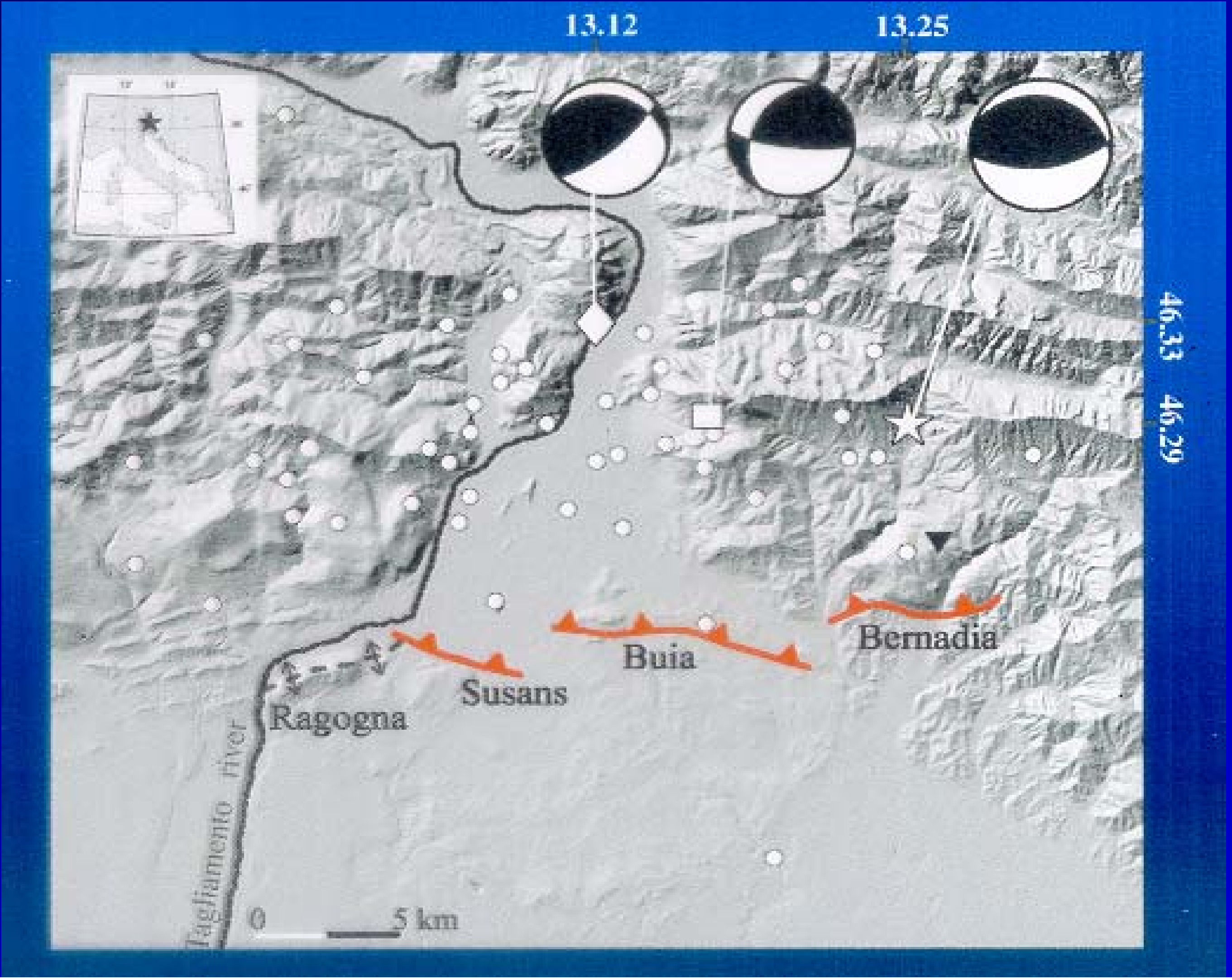

The 1976 Friuli Thrust-faulting Earthquake, Ms 6.5

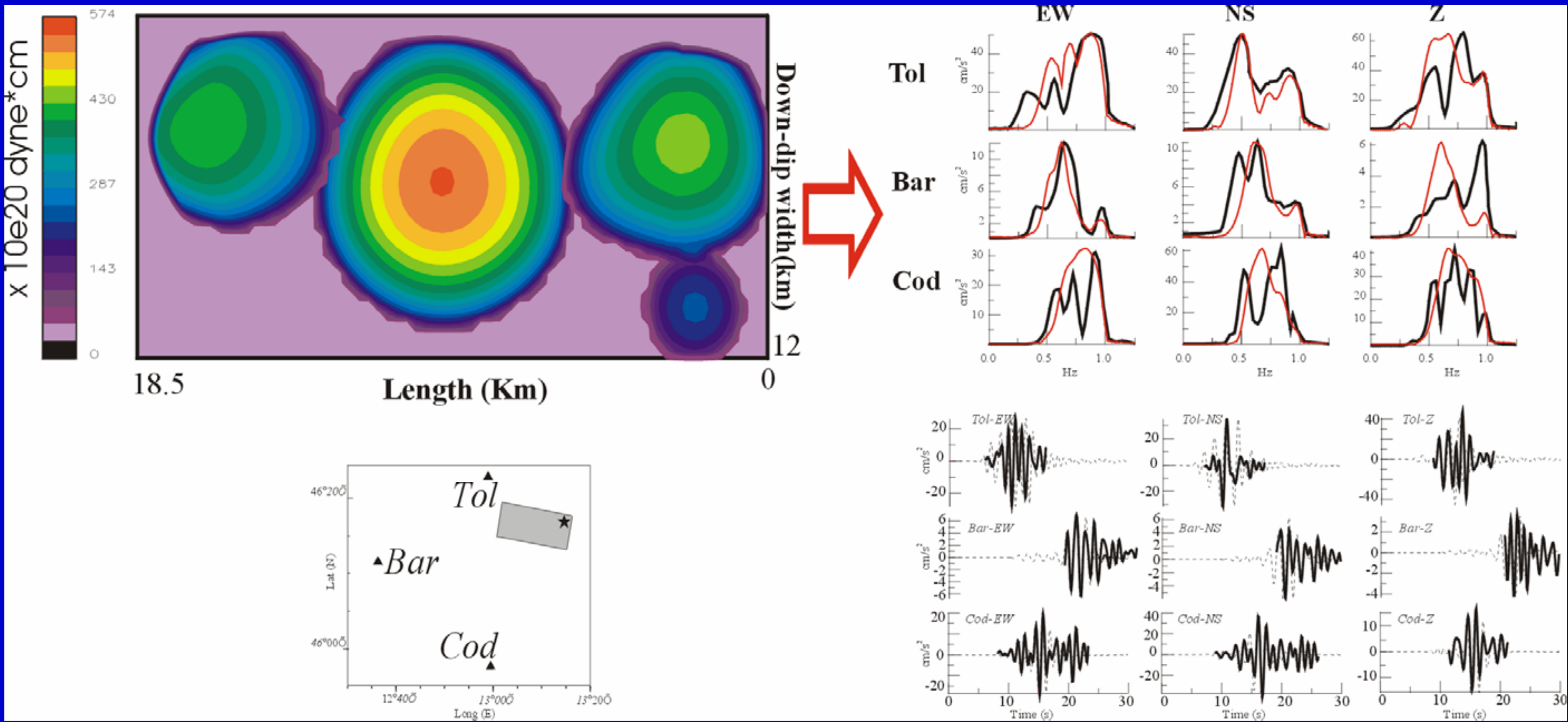

Inversion of the
Bovec 1998 (W Slovenia)
event

The Bovec-Krn (Slovenia) April 12, 1998 event

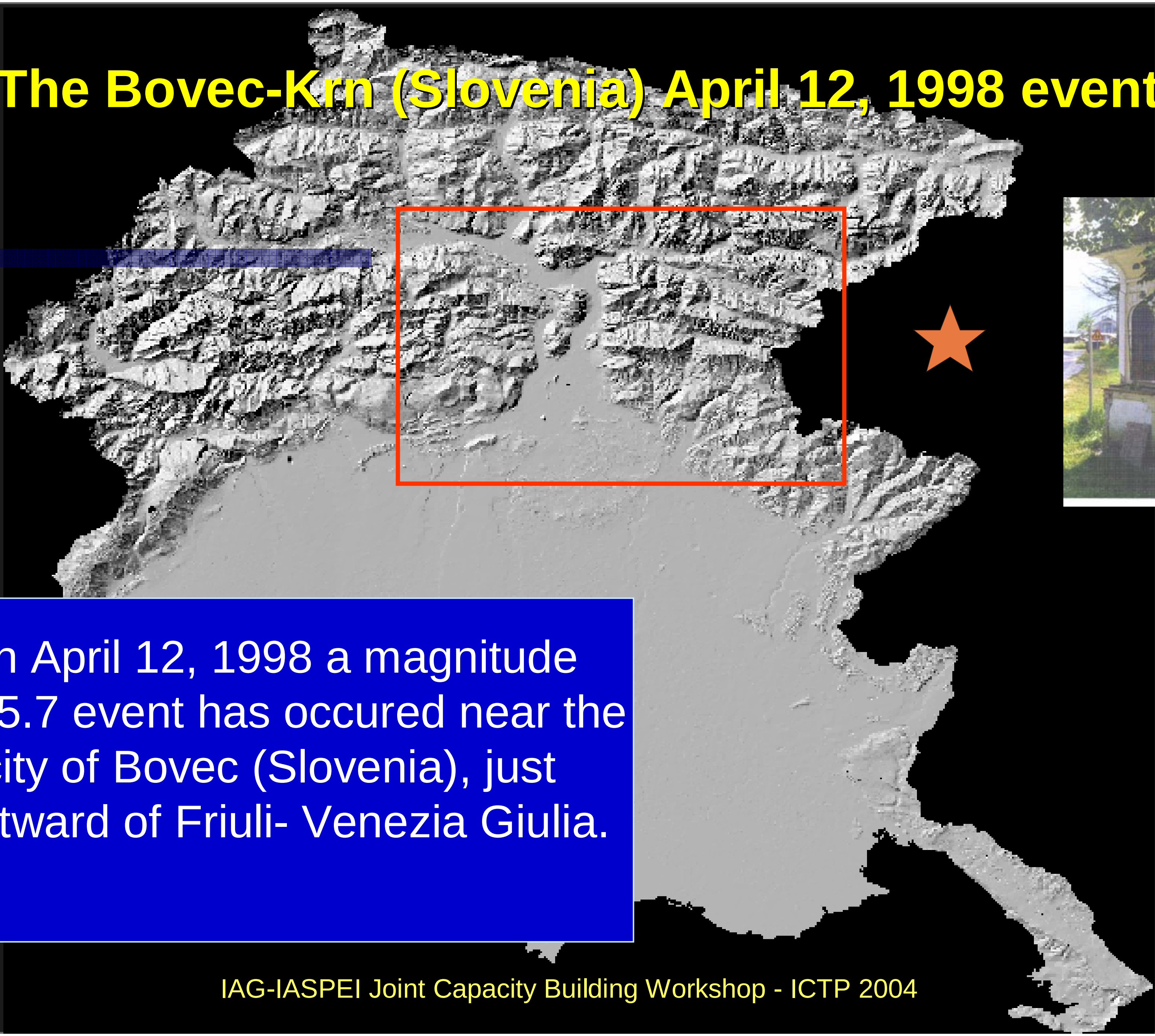

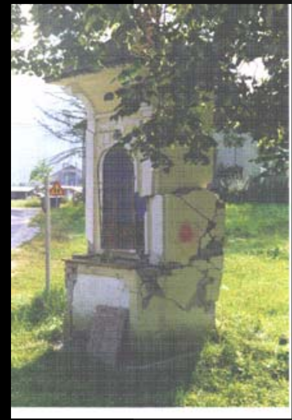

On April 12, 1998 a magnitude Ms=5.7 event has occured near the city of Bovec (Slovenia), just eastward of Friuli- Venezia Giulia.

Bovec 1998 - Locations

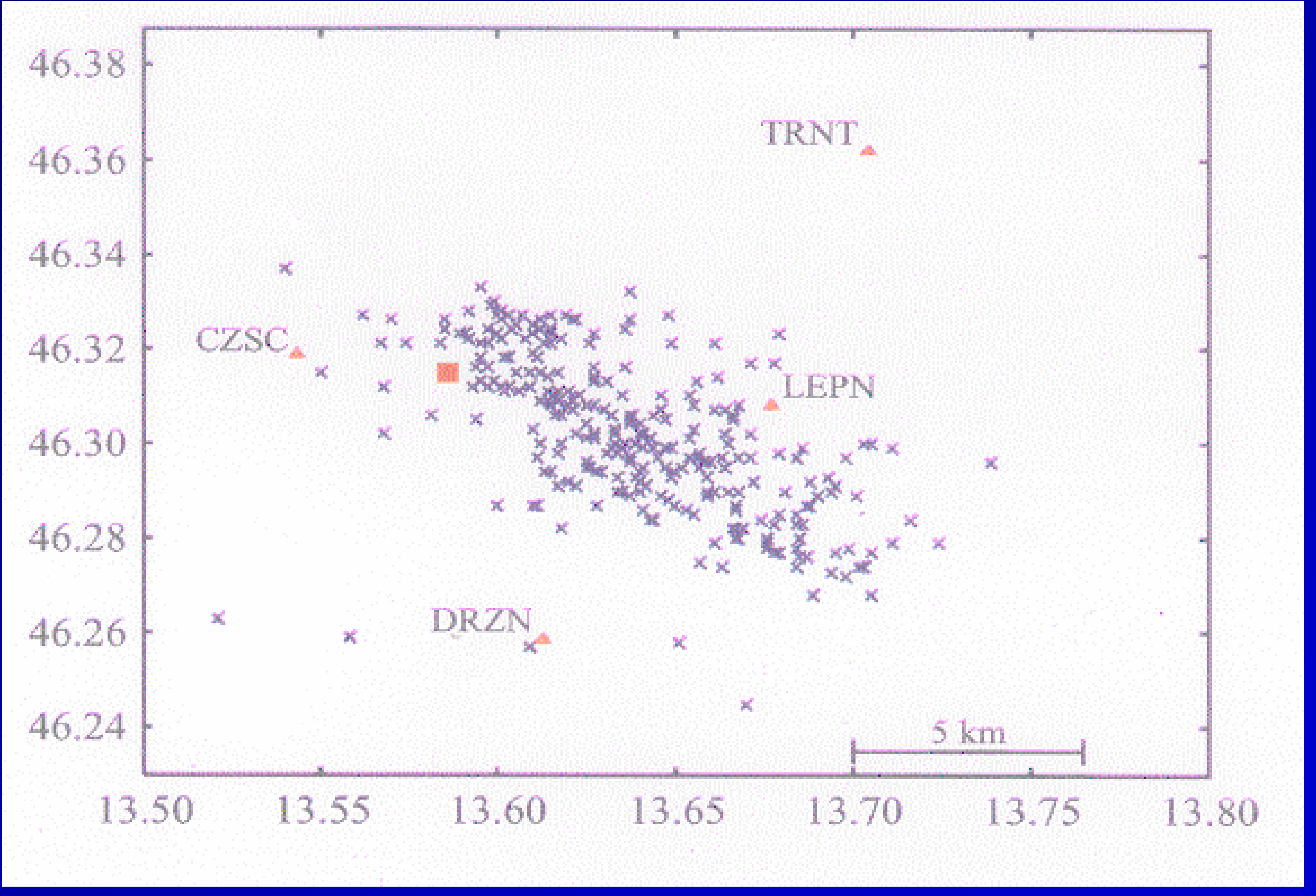

Bovec 1998 - Relocations

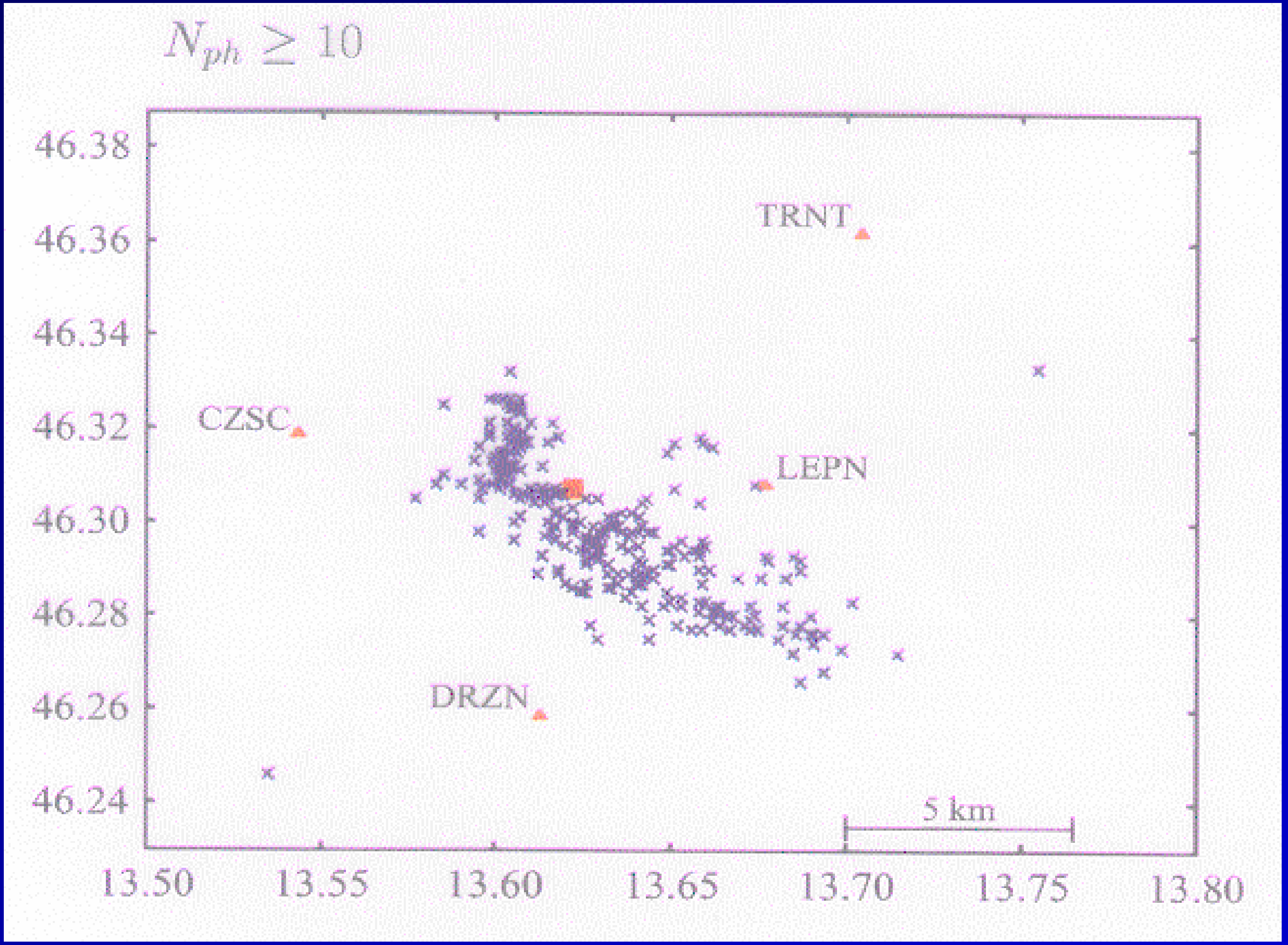

Bovec 1998 - Relocation errors

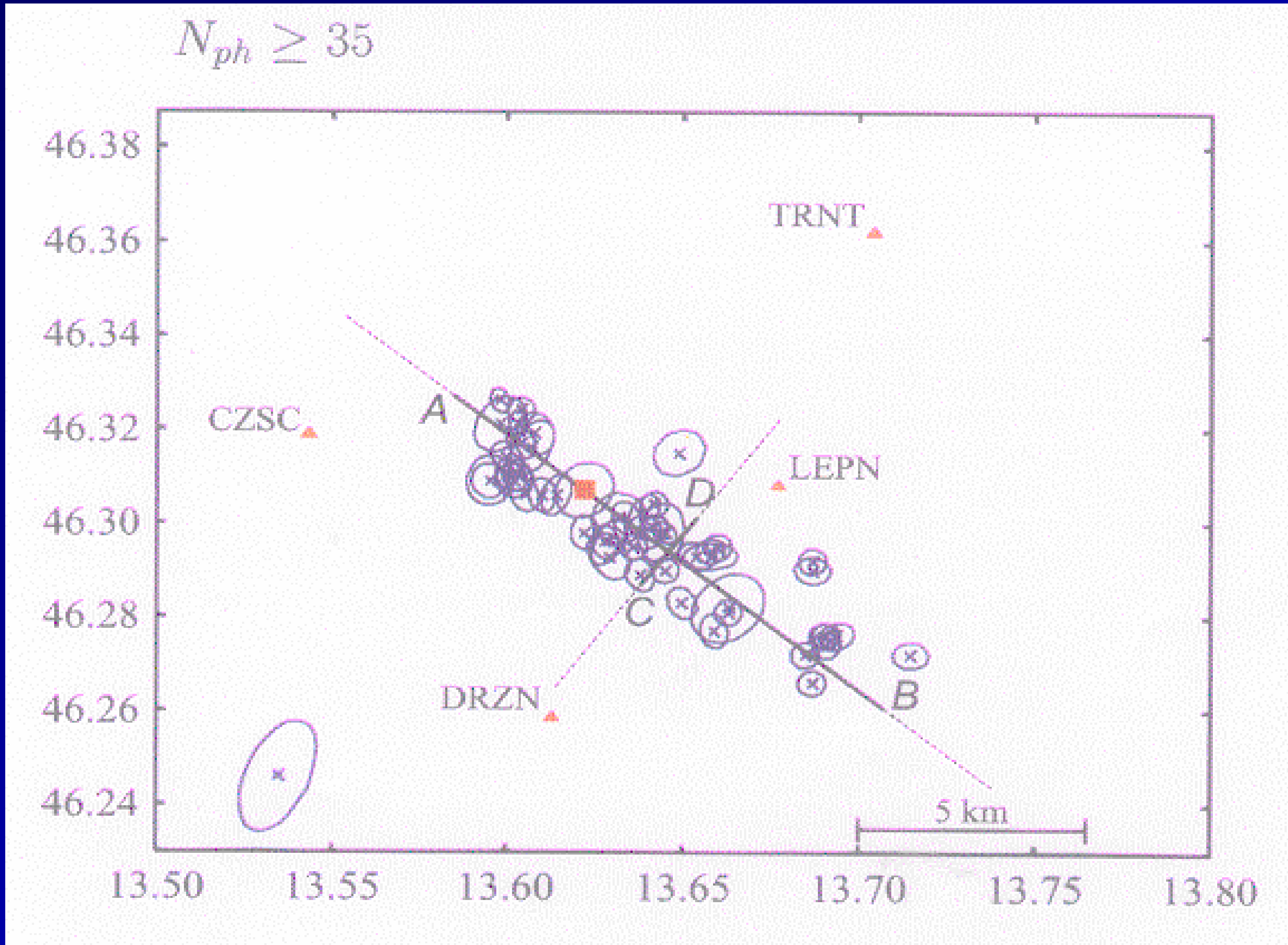

The 1998 Bovec earthquake sequence

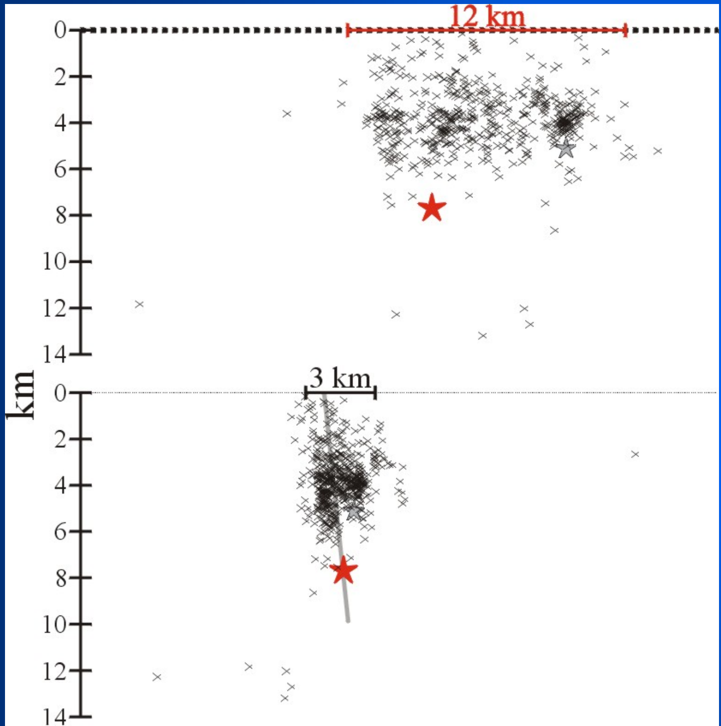

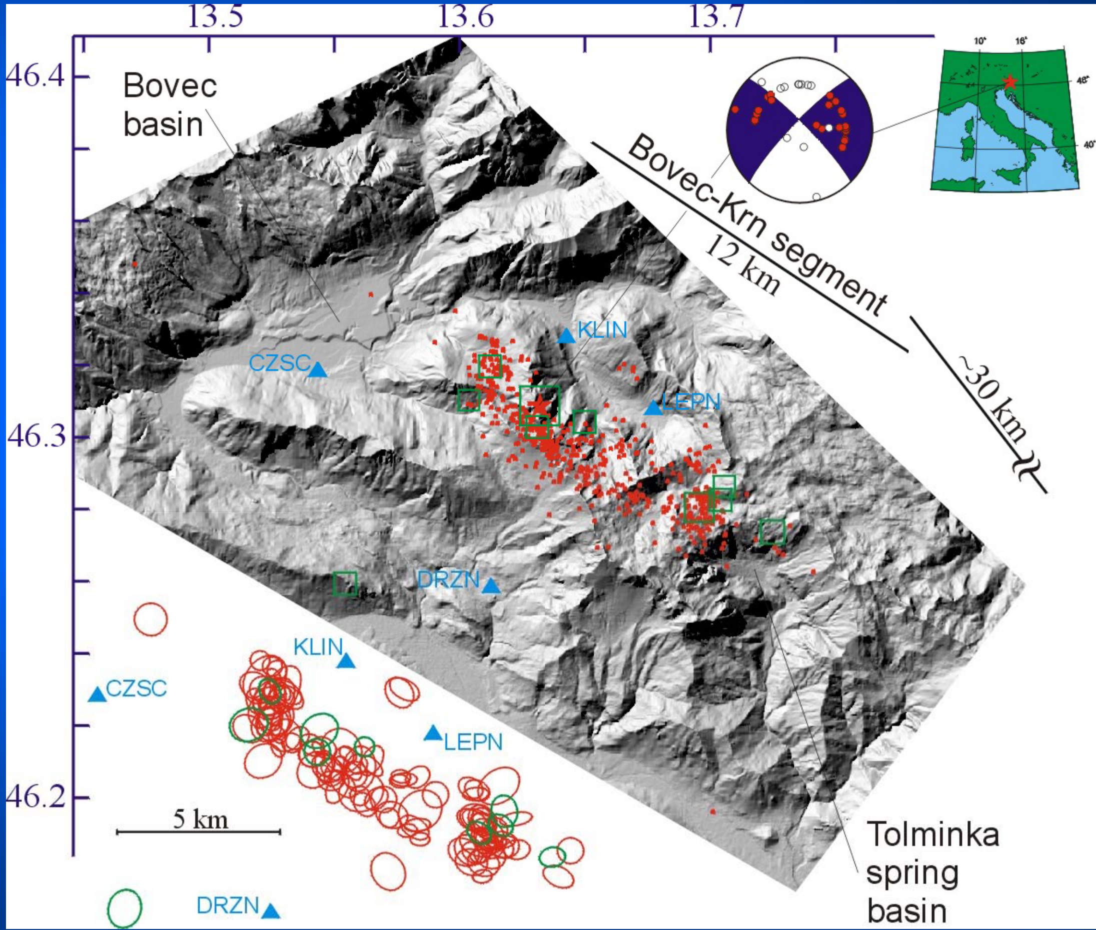

Filtering of data - max freq 1 Hz

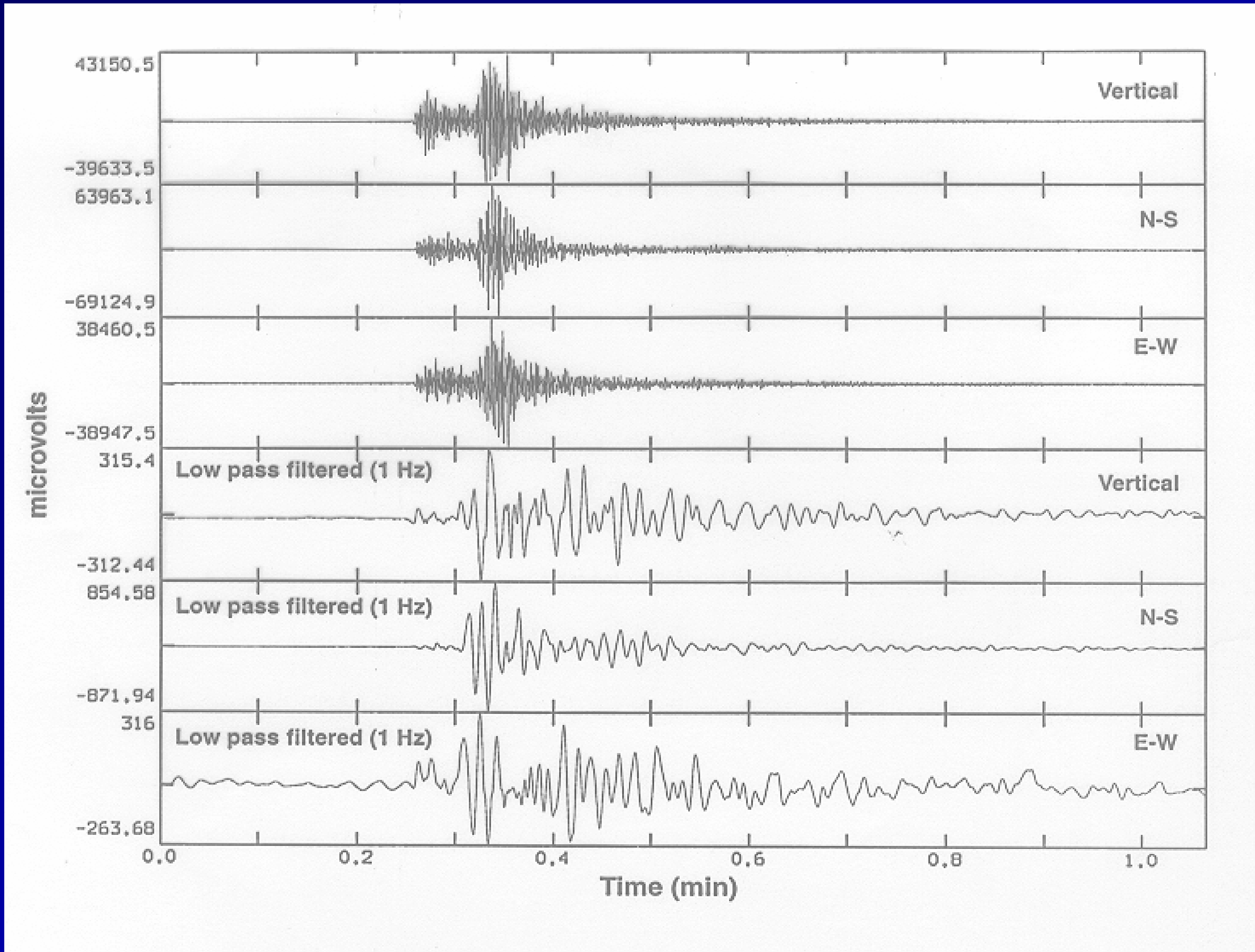

Which portion to invert?

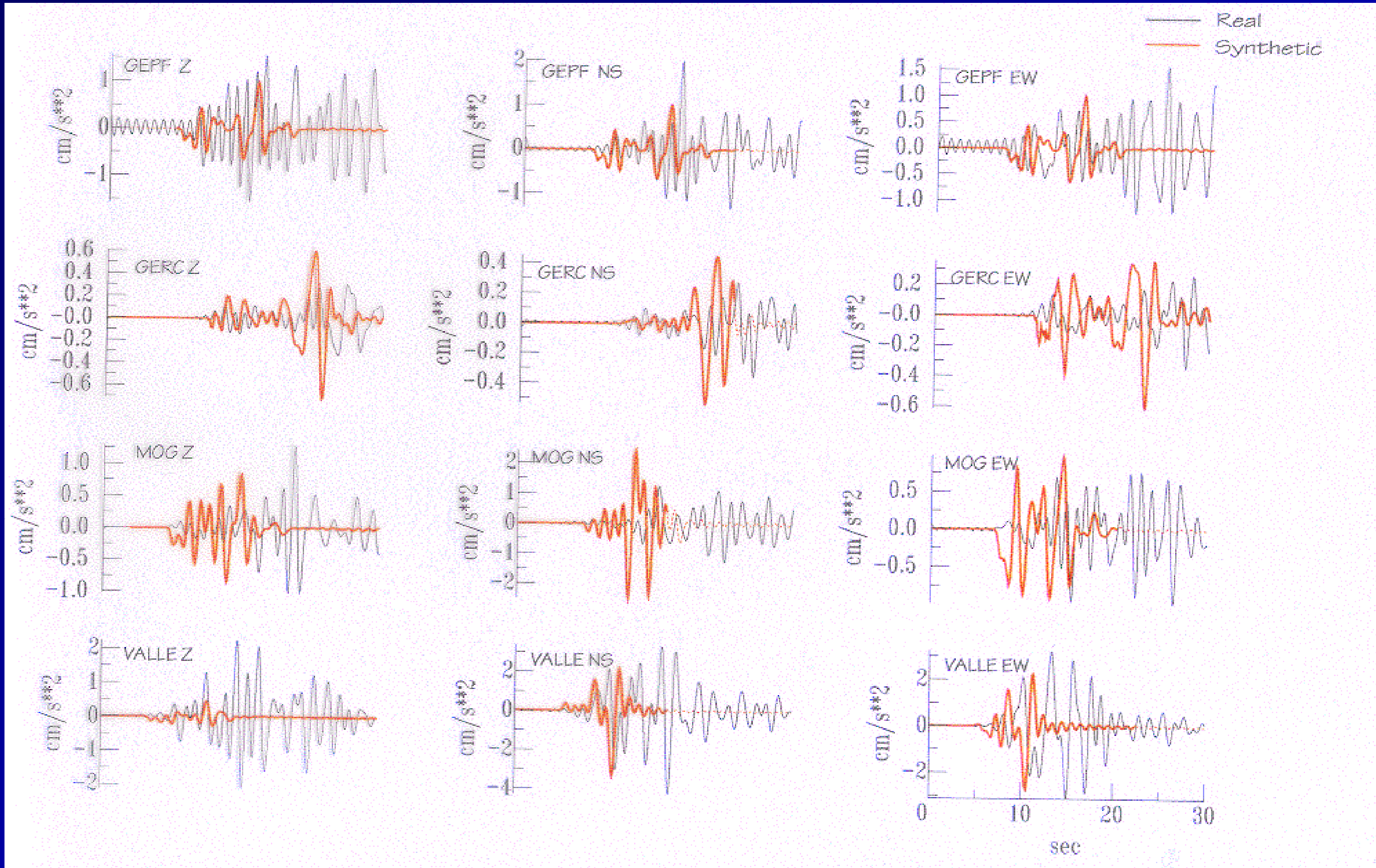

Model 1

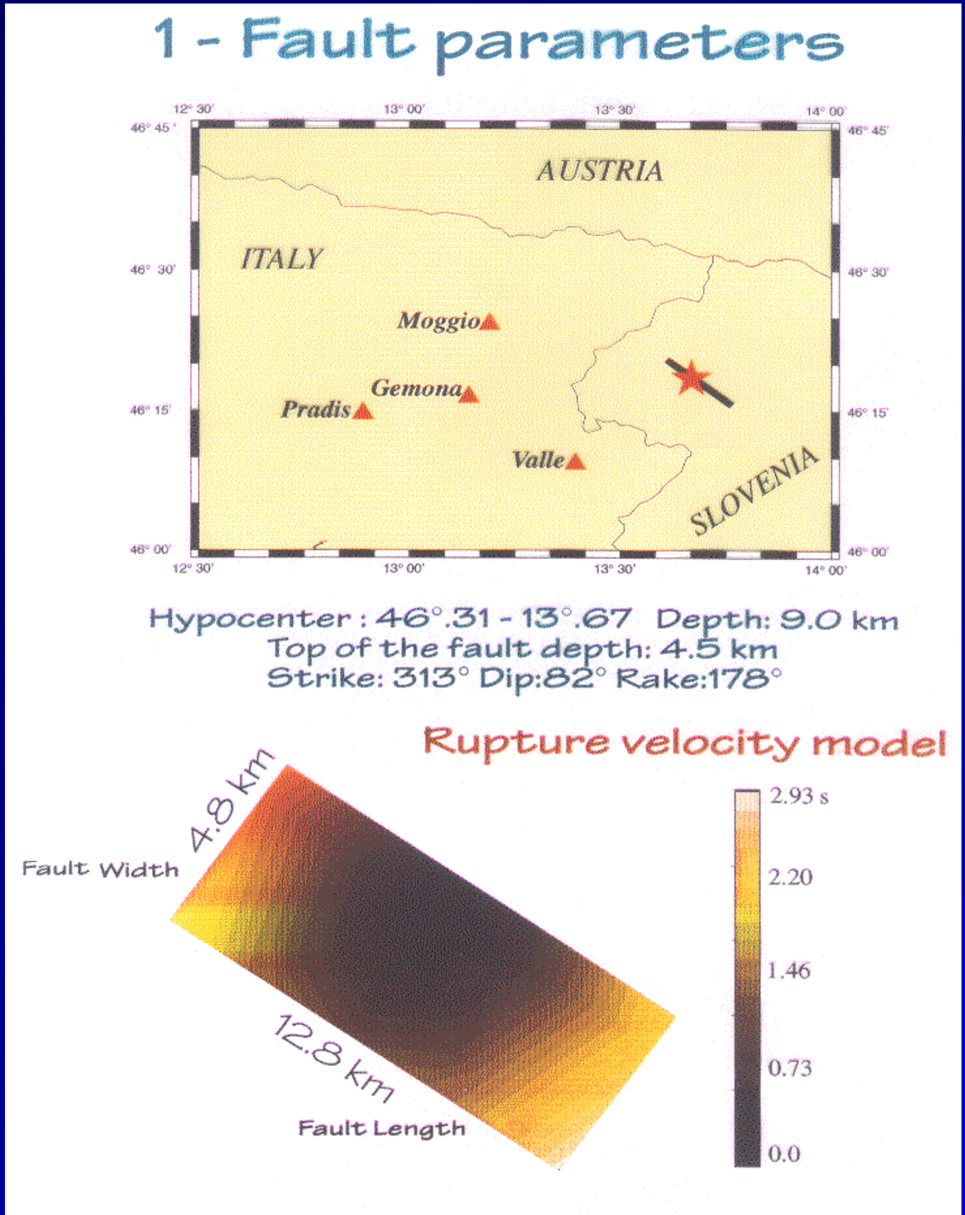

1 - Fault parameters
AUSTRIA
ITALY
Moggio
Gemona
Pradis
Valle
SLOVENIA
12° 30'
13° 00'
13° 30'
14° 00'
46° 45'
46° 30'
46° 15'
46° 00'
Hypocenter : 46°.31 - 13°.67 Depth: 9.0 km
Top of the fault depth: 4.5 km
Strike: 313° Dip:82° Rake:178°
Rupture velocity model
4.8 km
Fault Width
12.8 km
Fault Length
2.93 s
2.20
1.46
0.73
0.0

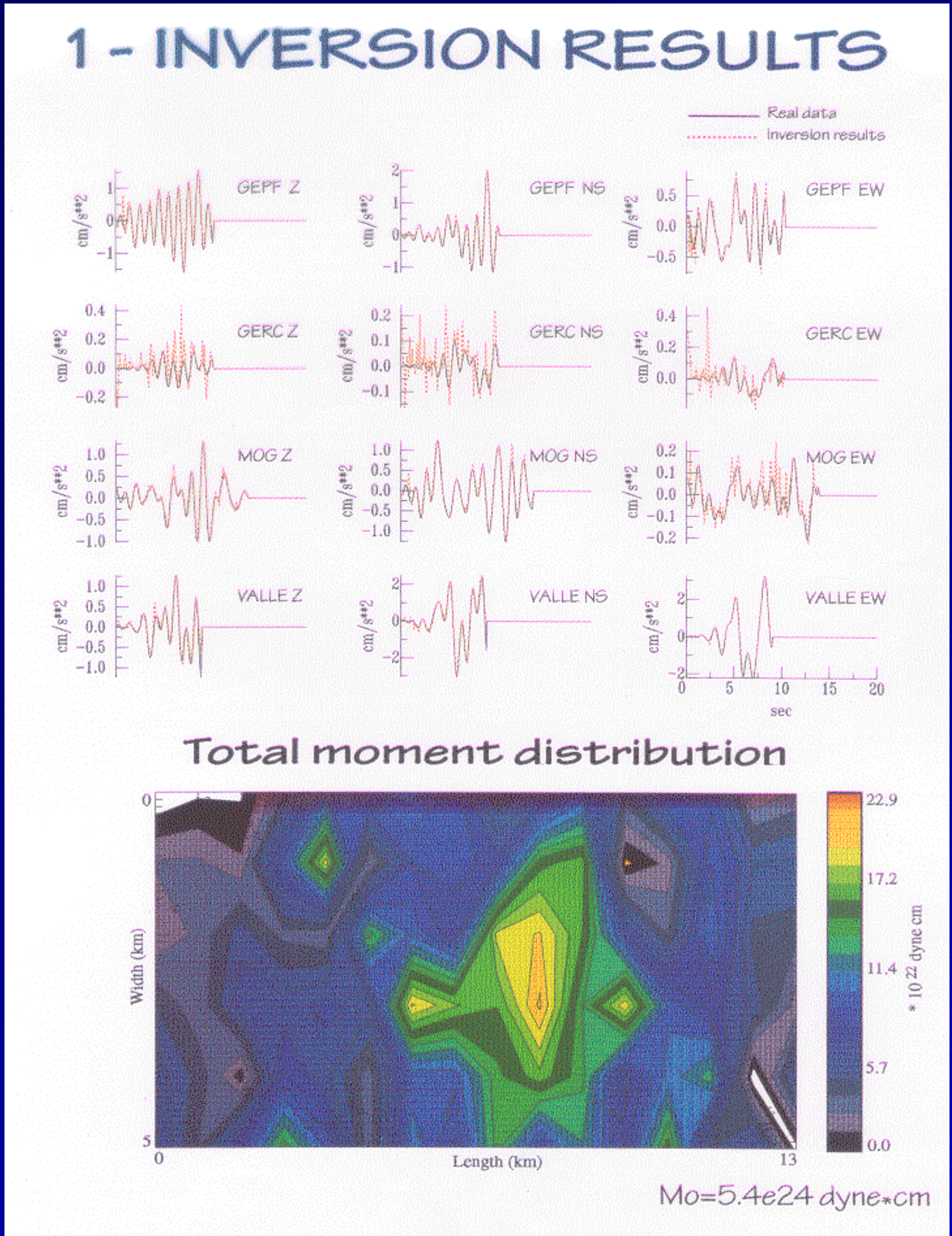
1 - INVERSION RESULTS
Real data
Inversion results
GEPF Z
GEPF NS
GEPF EW
GERC Z
GERC NS
GERC EW
MOG Z
MOG NS
MOG EW
VALLE Z
VALLE NS
VALLE EW
cm/s**2
sec
Total moment distribution
Width (km)
Length (km)
* 10 22 dyne cm
Mo=5.4e24 dyne*cm

Model 1

Model 2

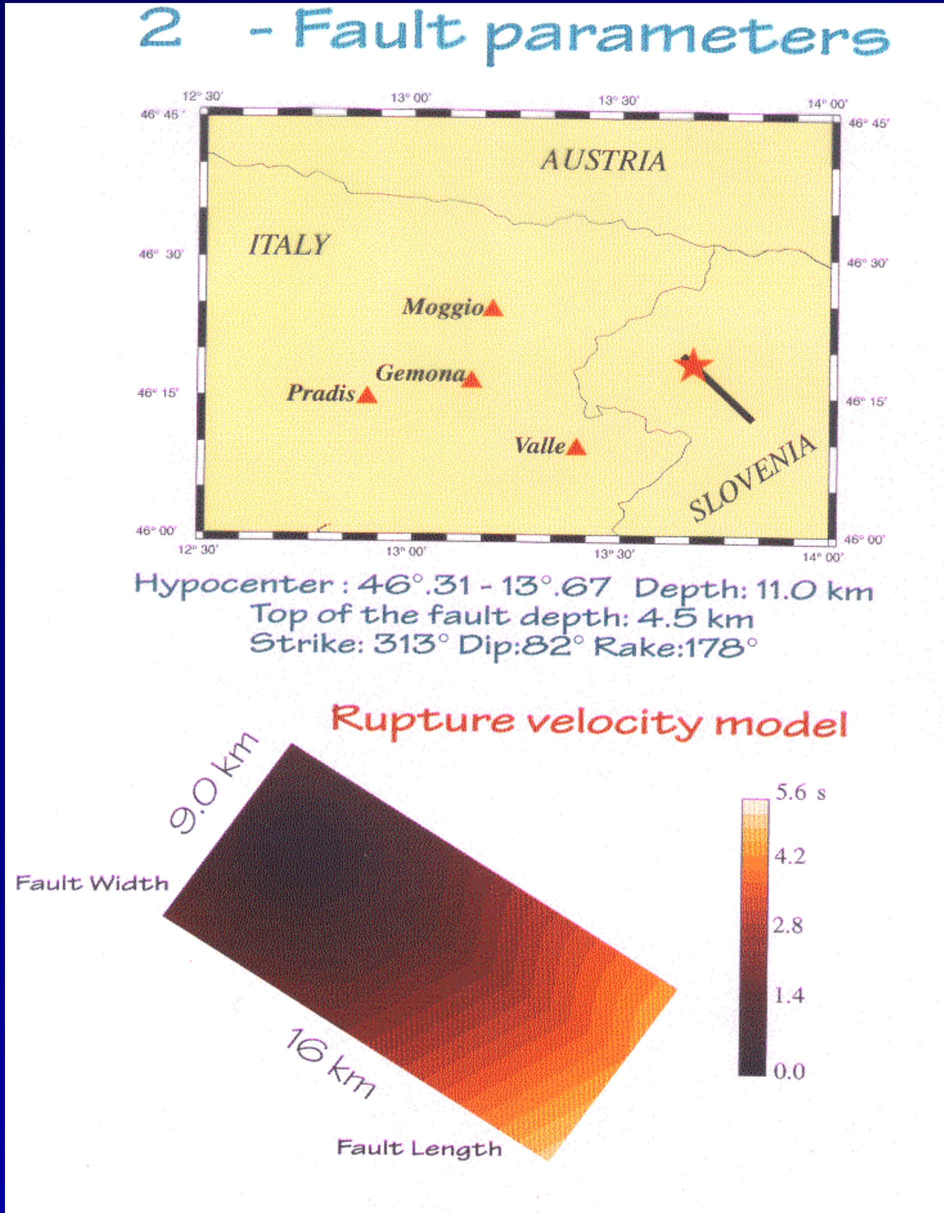

2 - Fault parameters
AUSTRIA
ITALY
Moggio
Gemona
Pradis
Valle
SLOVENIA
Hypocenter : 46°.31 - 13°.67 Depth: 11.0 km
Top of the fault depth: 4.5 km
Strike: 313° Dip:82° Rake:178°
Rupture velocity model
9.0 km
Fault Width
16 km
Fault Length
5.6 s
4.2
2.8
1.4
0.0

Model 2

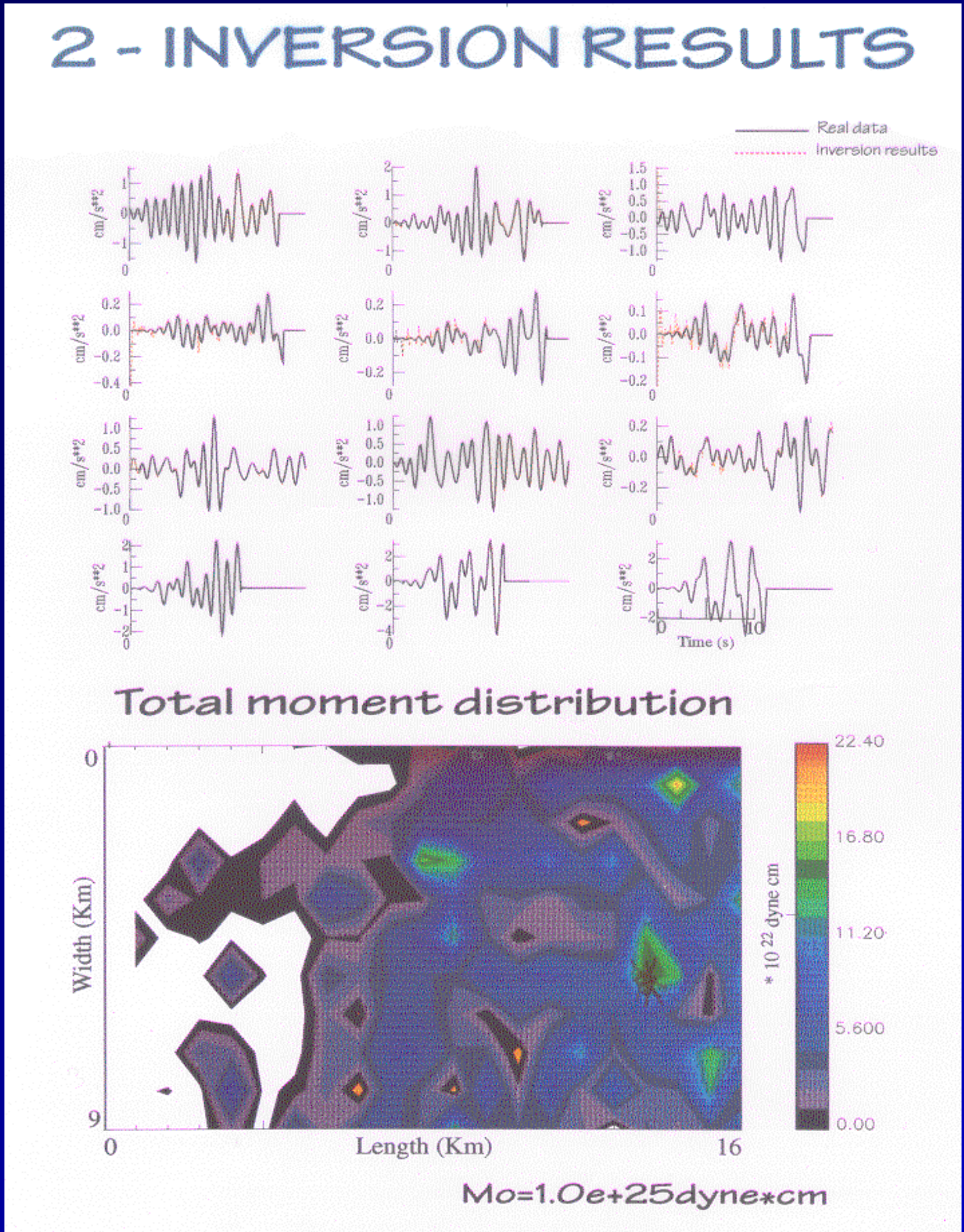
2 - INVERSION RESULTS
Real data
Inversion results
cm/s**2
Time (s)
Total moment distribution
Width (Km)
Length (Km)
* 10 22 dyne cm
22.40
16.80
11.20
5.600
0.00
Mo=1.0e+25dyne*cm

Model 3

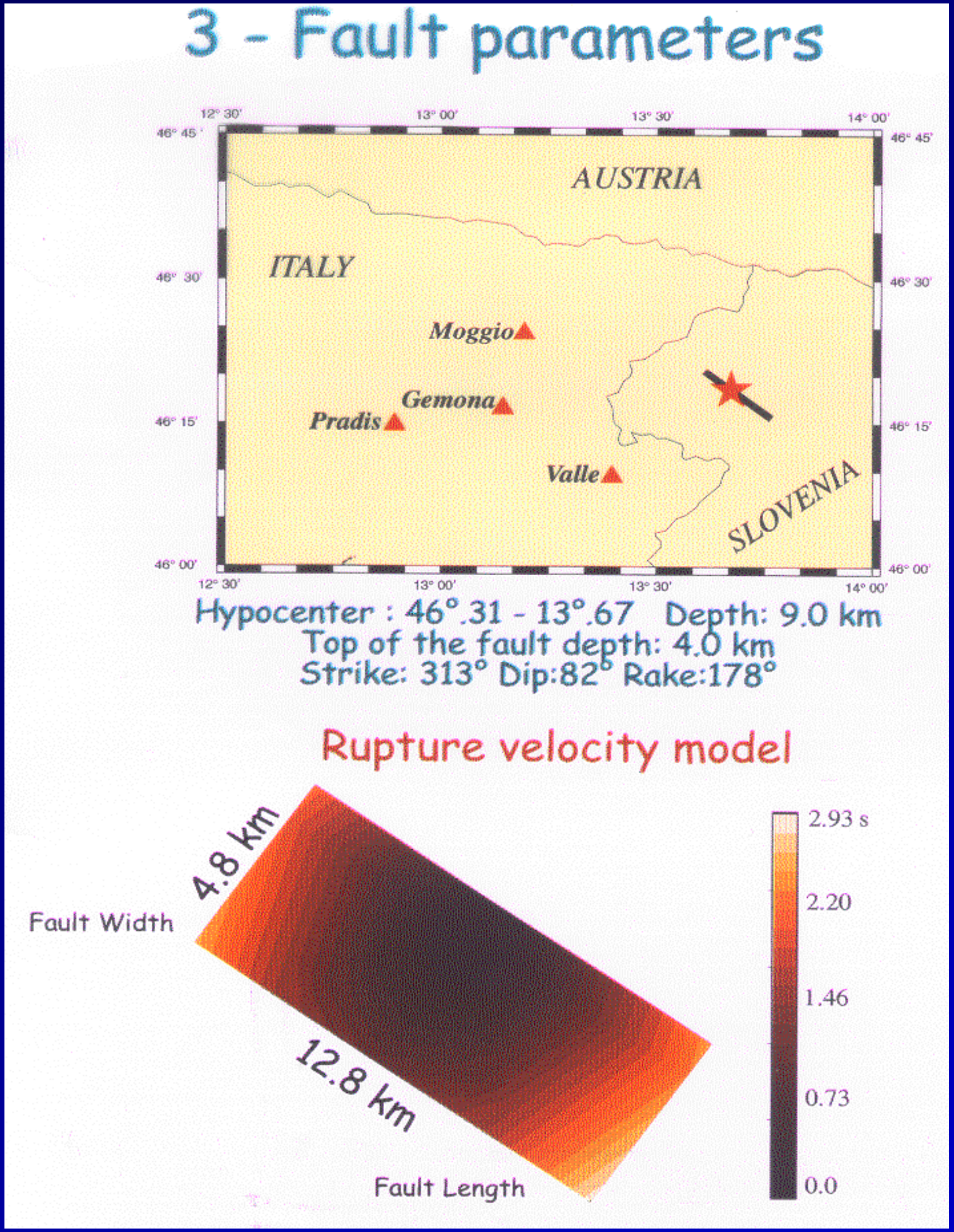
3 - Fault parameters
AUSTRIA
ITALY
Moggio
Gemona
Pradis
Valle
SLOVENIA
Hypocenter : 46°.31 - 13°.67 Depth: 9.0 km
Top of the fault depth: 4.0 km
Strike: 313° Dip:82° Rake:178°
Rupture velocity model
4.8 km
Fault Width
12.8 km
Fault Length
2.93 s
2.20
1.46
0.73
0.0

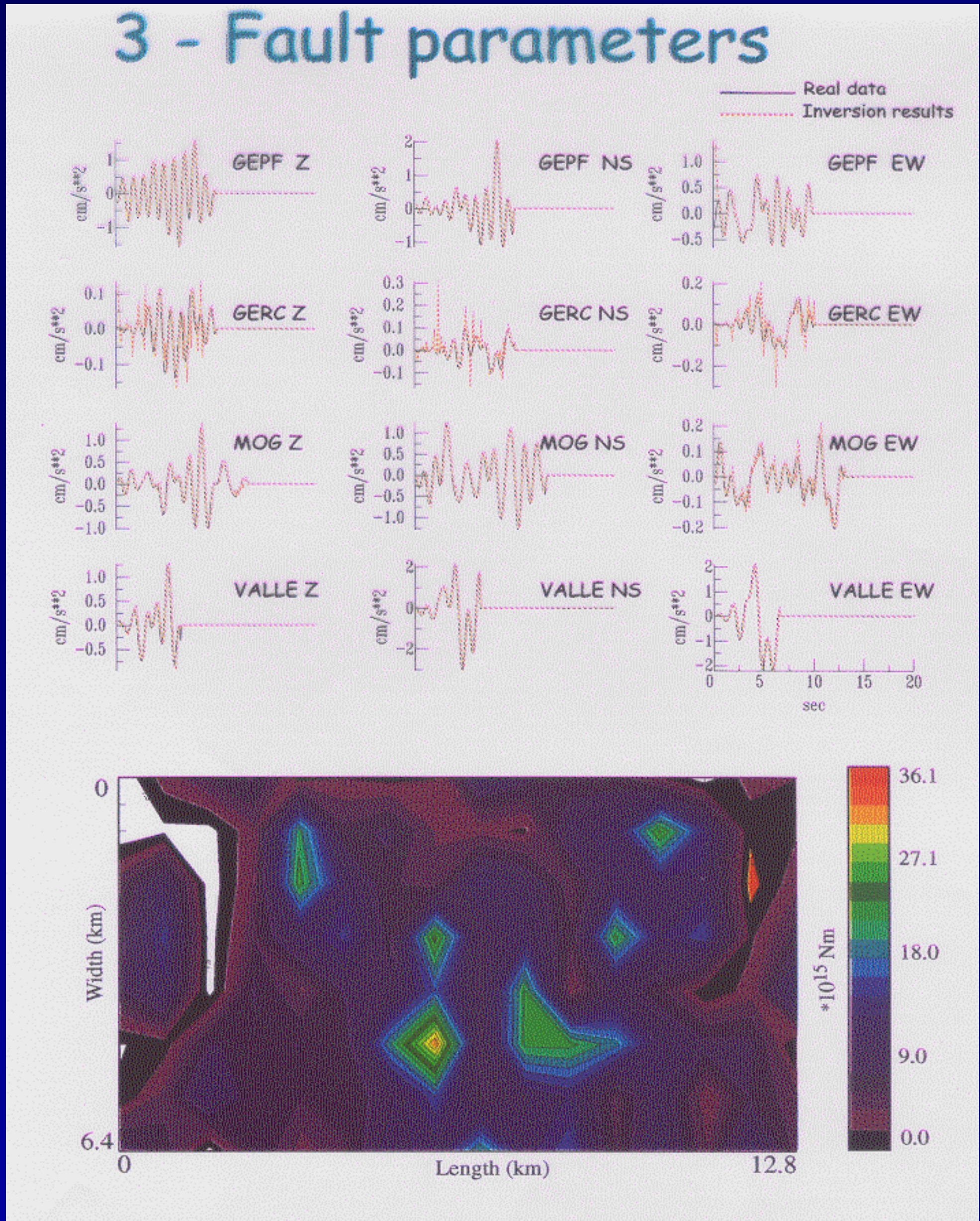

3 - Fault parameters
Real data
Inversion results
GEPF Z
GEPF NS
GEPF EW
GERC Z
GERC NS
GERC EW
MOG Z
MOG NS
MOG EW
VALLE Z
VALLE NS
VALLE EW
cm/s**2
sec
Width (km)
Length (km)
*10^15 Nm
36.1
27.1
18.0
9.0
0.0
0
6.4
12.8

Model 3

Final

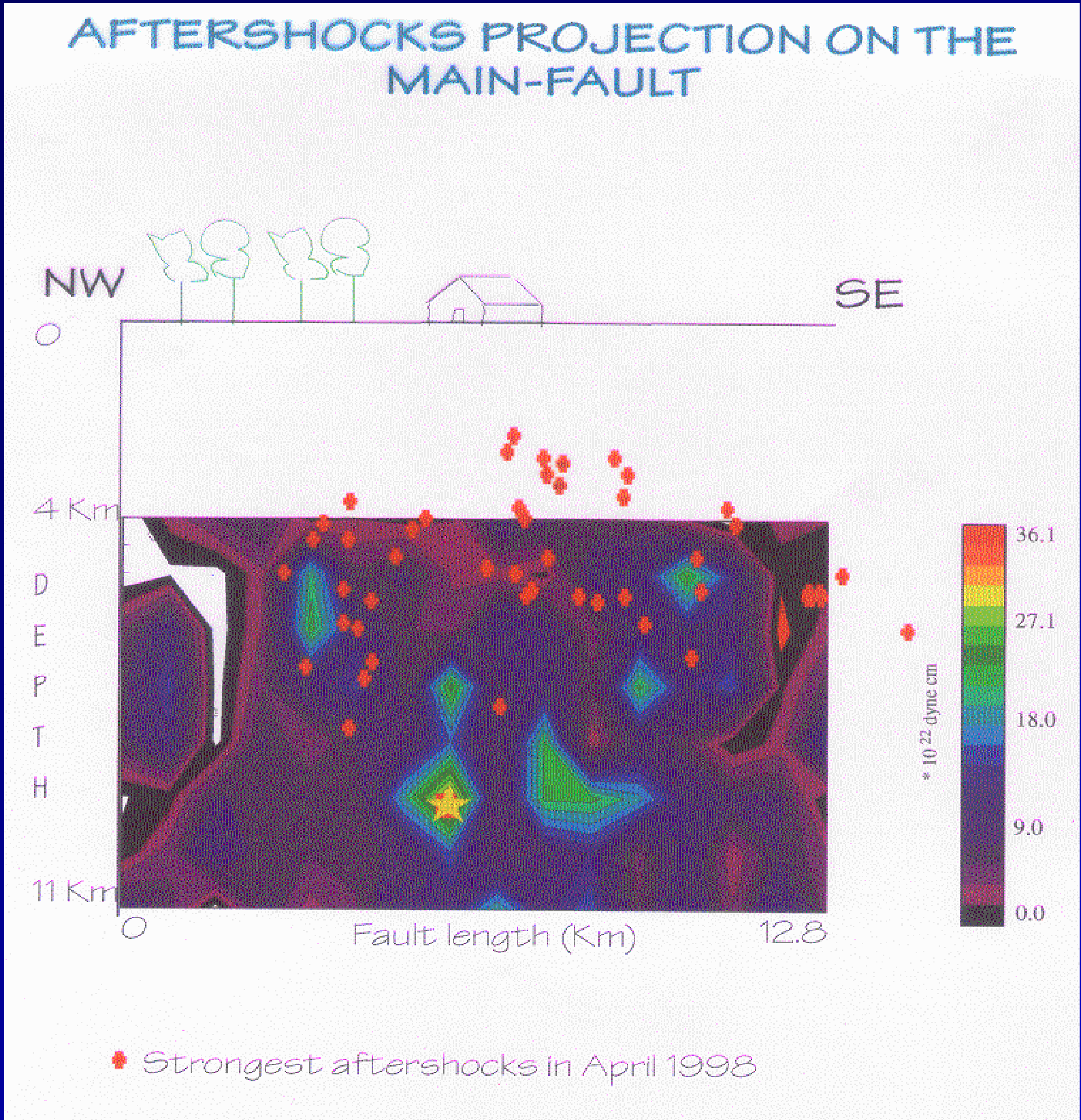

AFTERSHOCKS PROJECTION ON THE MAIN-FAULT
NW
SE
0
4 Km
DEPTH
11 Km
0
Fault length (Km)
12.8
36.1
27.1
18.0
9.0
0.0
* 10 22 dyne cm
Strongest aftershocks in April 1998

Active Structures

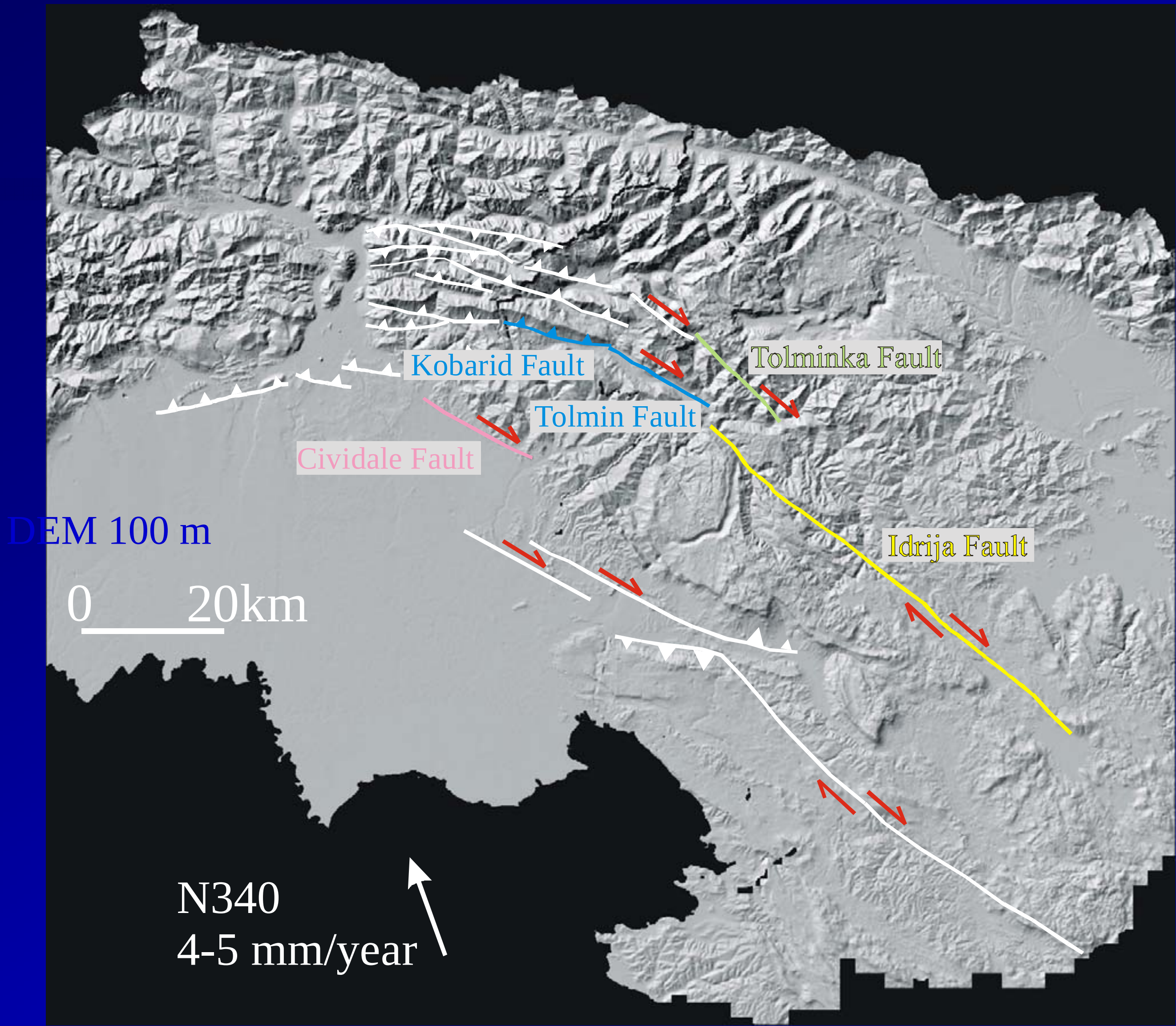

Slide

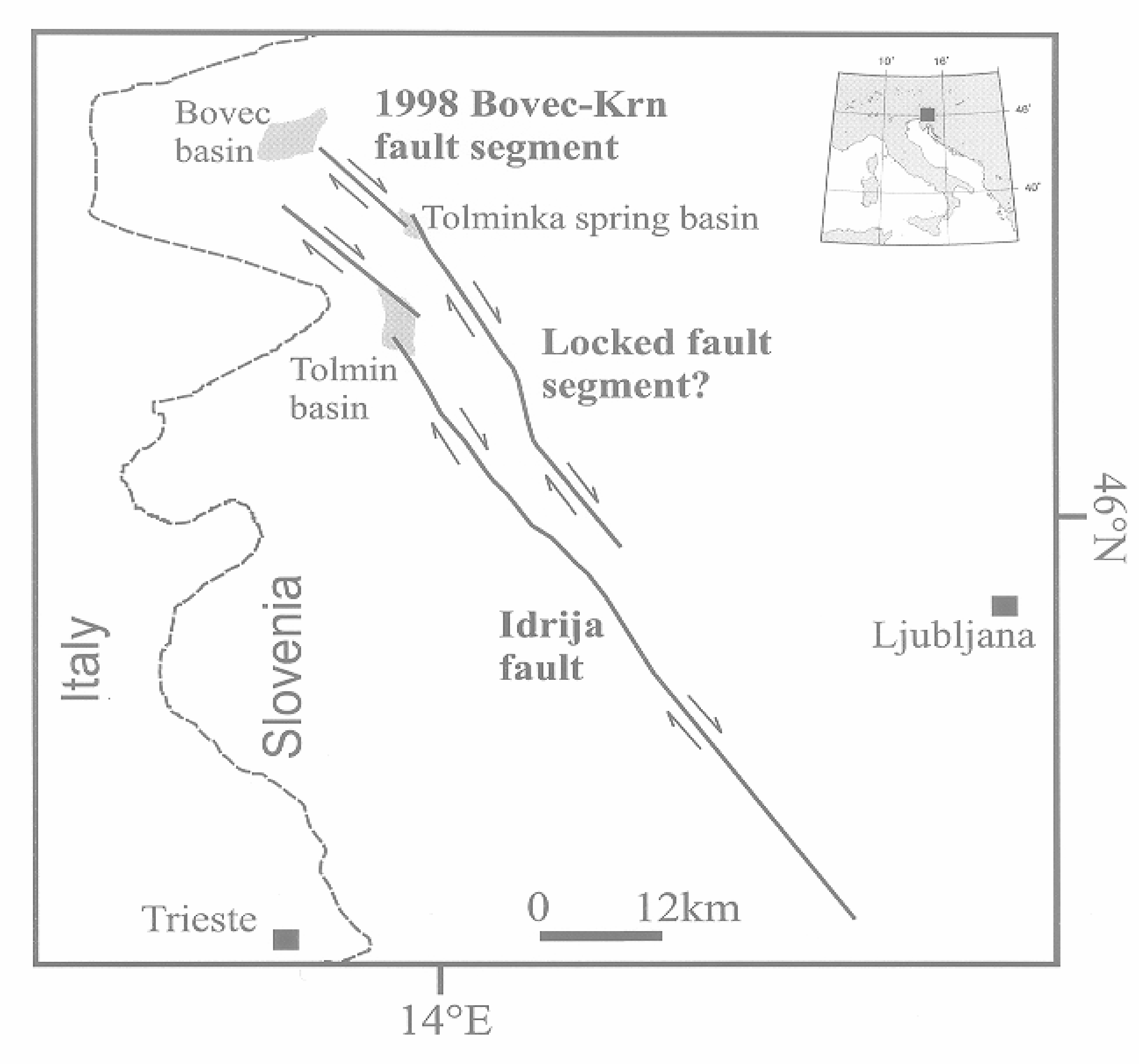
1998 Bovec-Krn
fault segment
Bovec
basin
Tolminka spring basin
Locked fault
segment?
Tolmin
basin
Italy
Slovenia
Idrija
fault
Ljubljana
46°N
Trieste
0
12km
14°E

Coulomb stress change

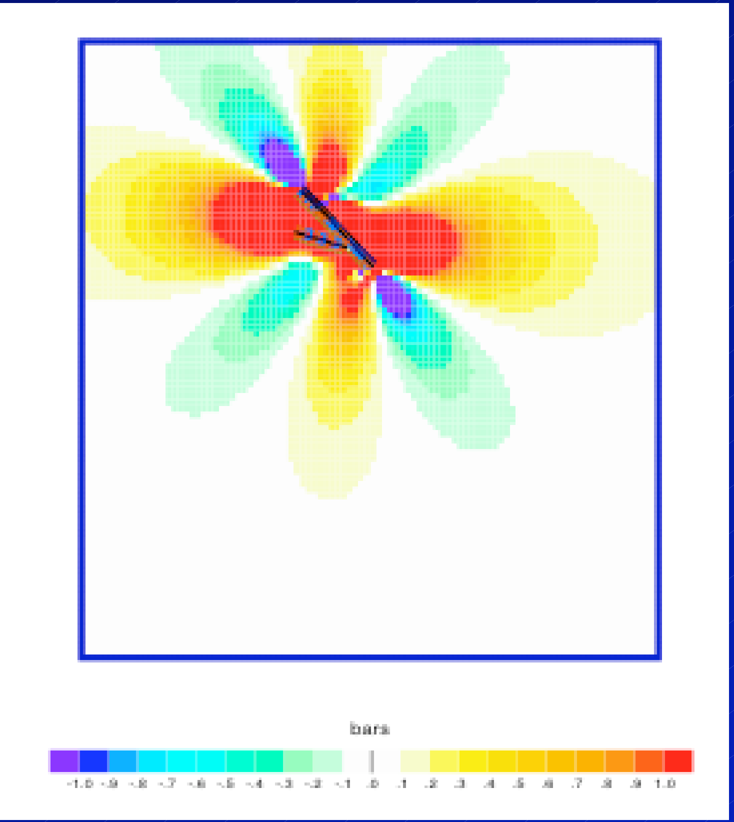

After 1998 event modeled with finite fault model of Bajc et al. (2002)

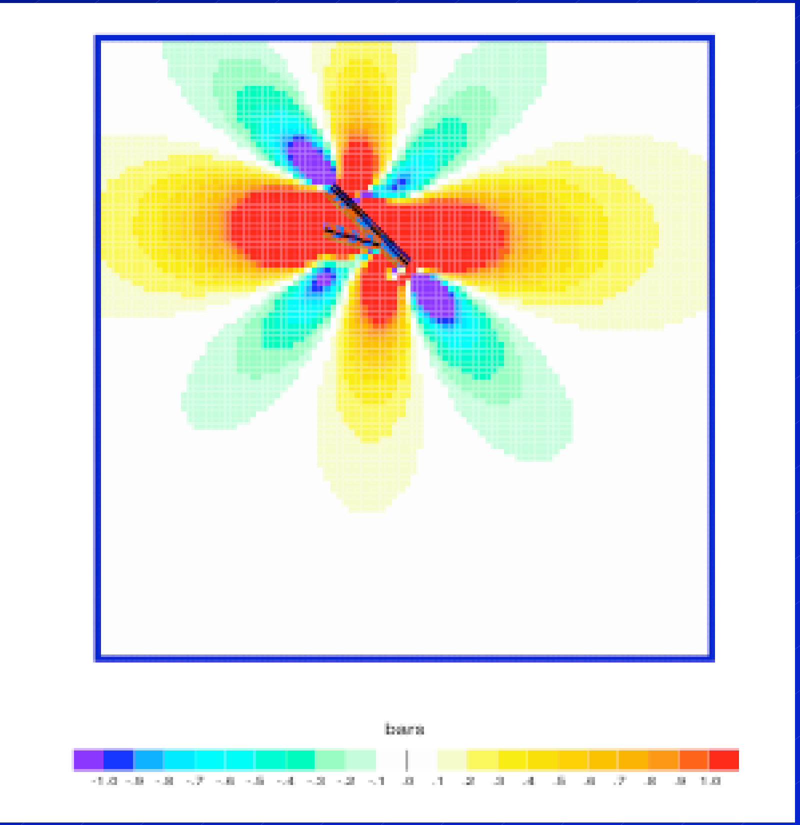

After 1998 and 2004 events: modeled with finite fault models of Bajc et al. (2002) and with uniform slip

Which active fault will rupture next?

The Coulomb stress change would thus favour an increased stress on the Kobarid-Tolmin fault and a reduced stress on the Tolminka fault

Which will be the next ruptured fault depends however on the accumulated stress level on the two faults…

- **Hazard scenarios**

Realistic Strong Ground Motion Scenarios for Seismic Hazard Assessment Studies at the Alps-Dinarides Junction

Method

Active Tectonics

- Identification of the Structures
- Definition of the *Input Fault Model* (L, W, M, θ, δ, λ)

Synthetic Seismograms Computation (1 Hz, 2 Hz)

- Different Nucleation Points along the Fault
- Uniform and Non-Uniform Seismic Moment Distribution
- Modal Summation for Extended Sources (Panza, 1985; Panza and Suhadolc, 1987; Florsch at al., 1991, Sarao' et al., 1998; Panza et al., 2001)

1 Hz, Dense Grid of Receivers

Contour Maps of Expected Maximum Horizontal Velocities

2 Hz, Relevant Localities of the Area

Expected Maximum Horizontal Displacement, Velocity and Acceleration

Method

Uniform Tapered Seismic Moment Distribution

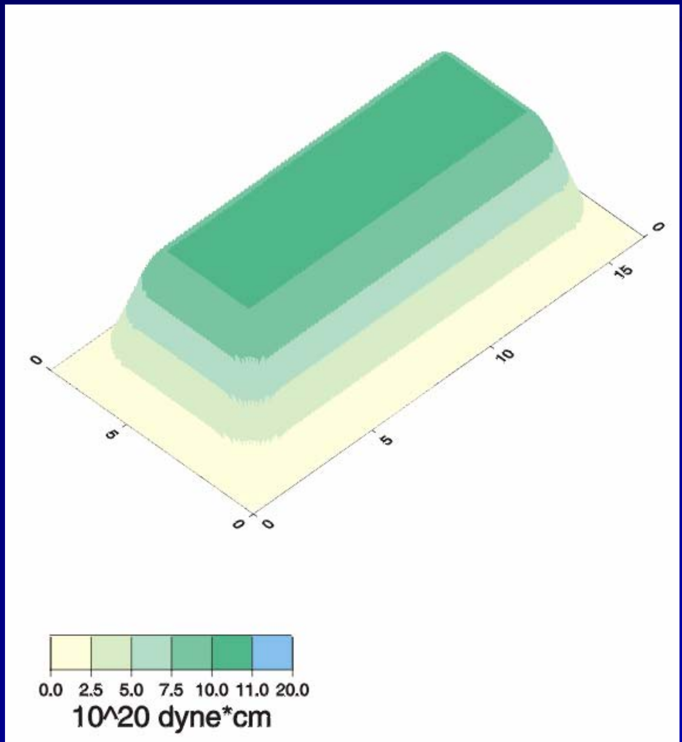

30% Tapering at the fault's edges

Non-Uniform Seismic Moment Distribution – The K^2 Model

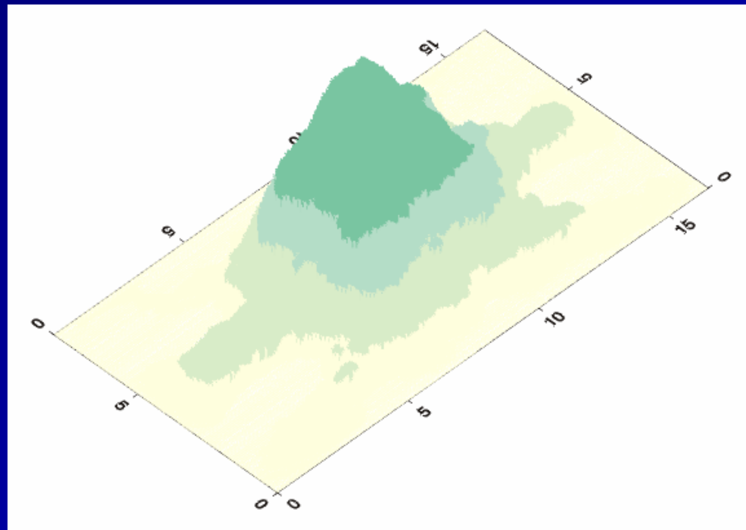

Single Asperity

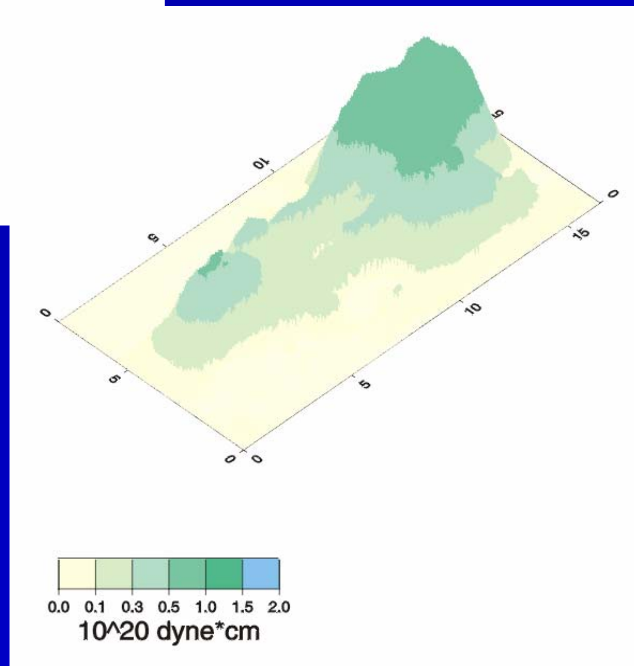

Double Asperity

Analyzed Active Structures

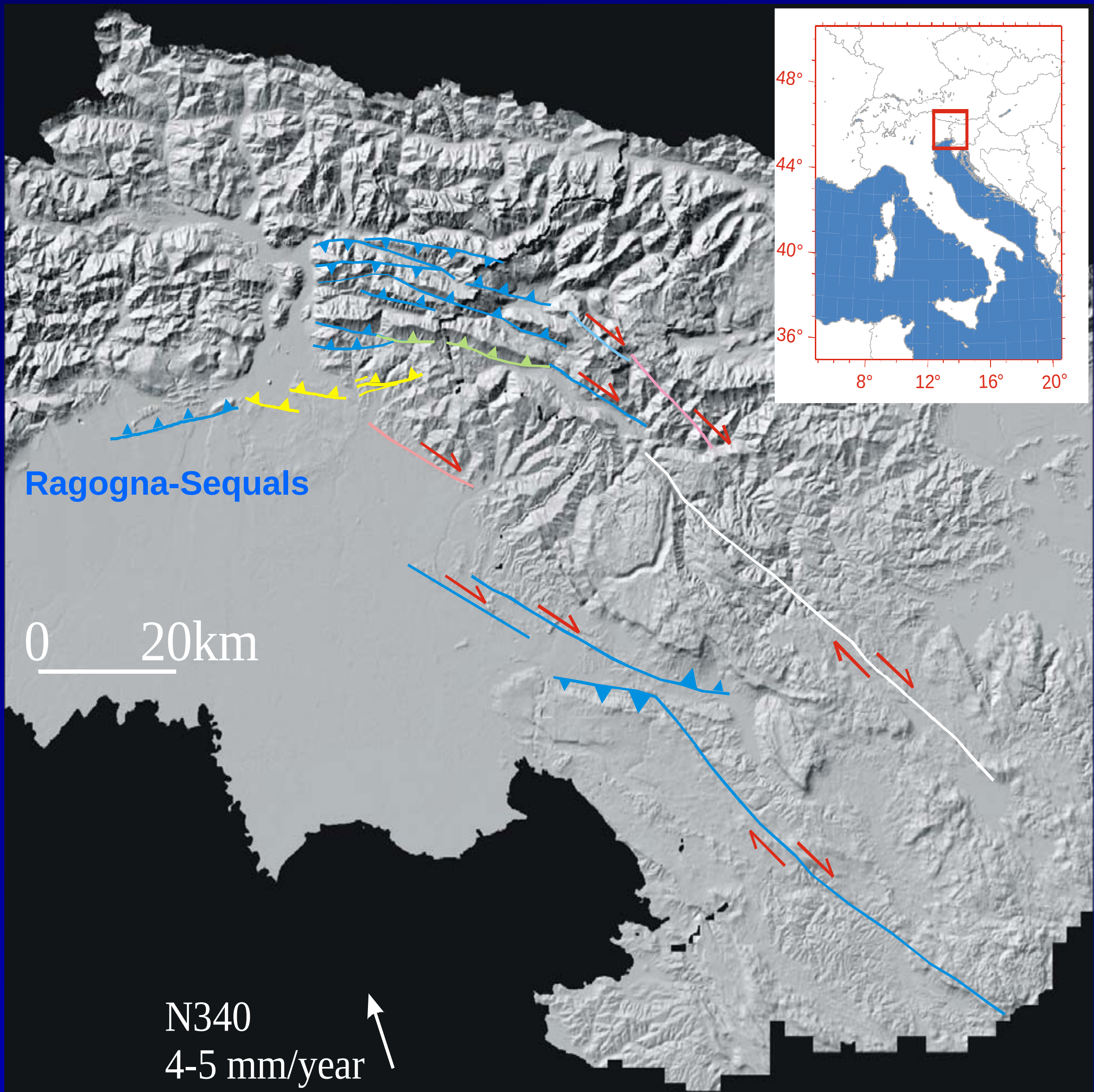

Leading edge of deformation

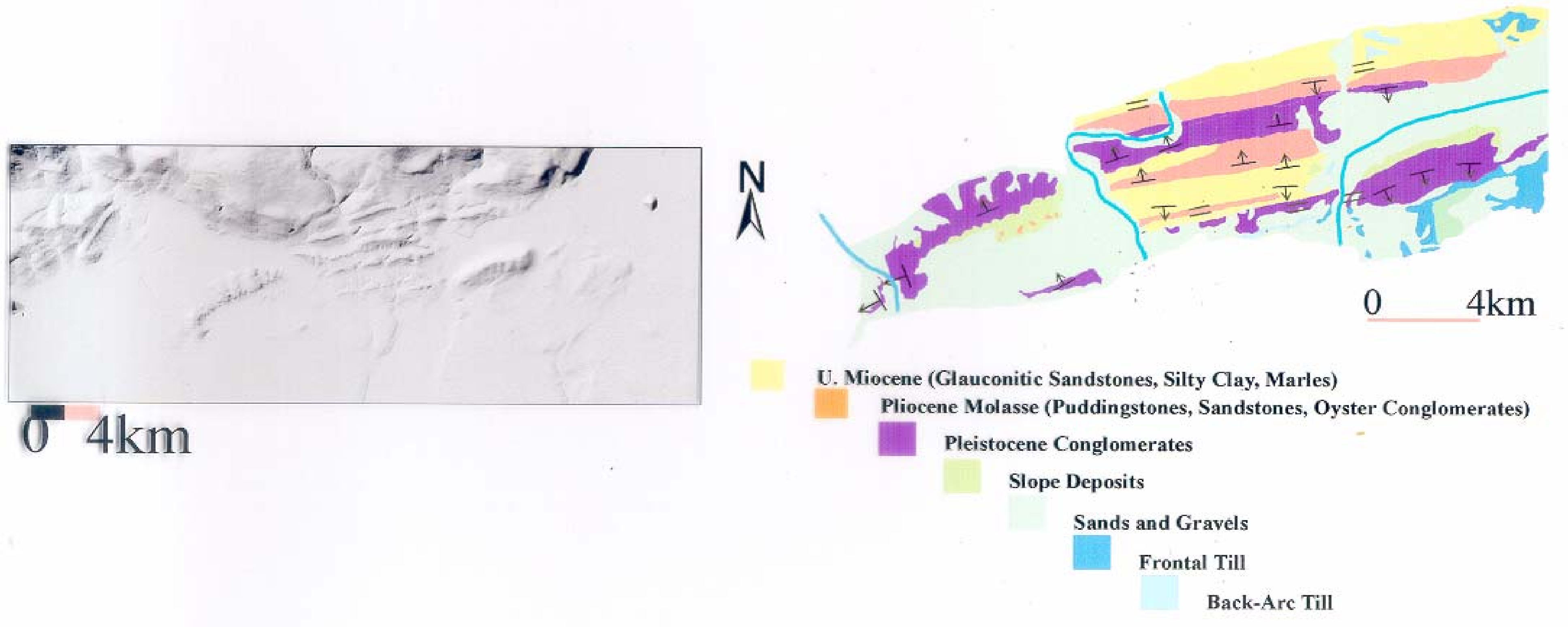

Ragogna-Sequals fault

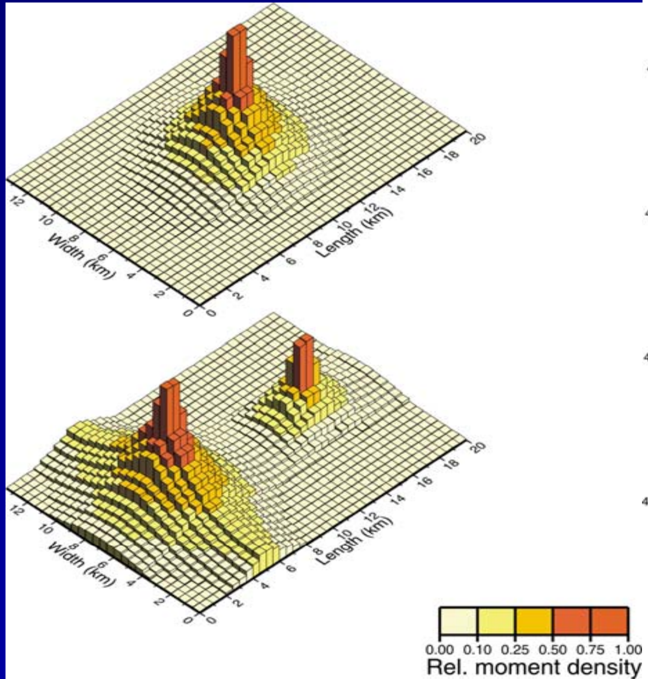

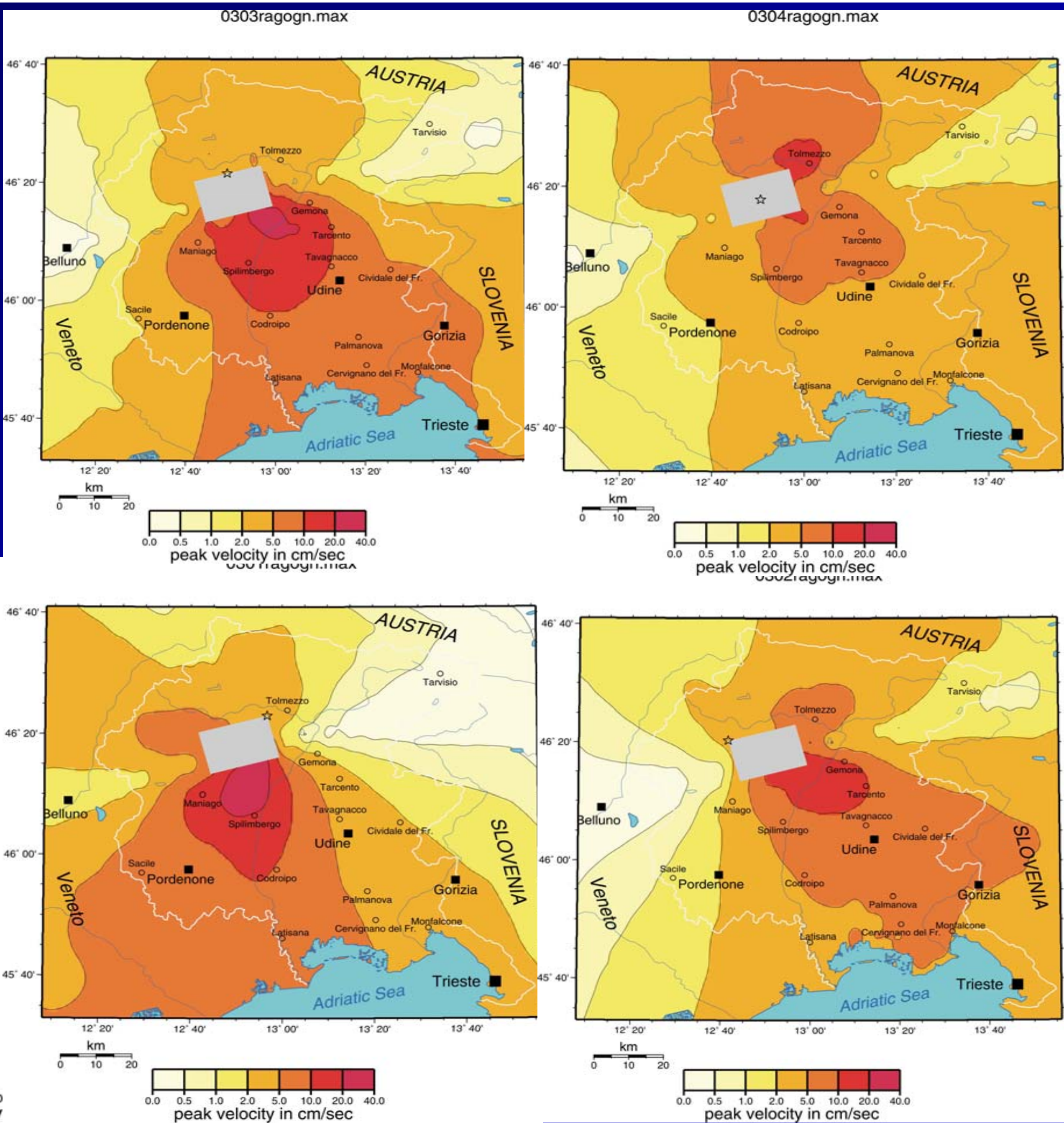

The Kobarid-Tolmin Fault (1 Hz):

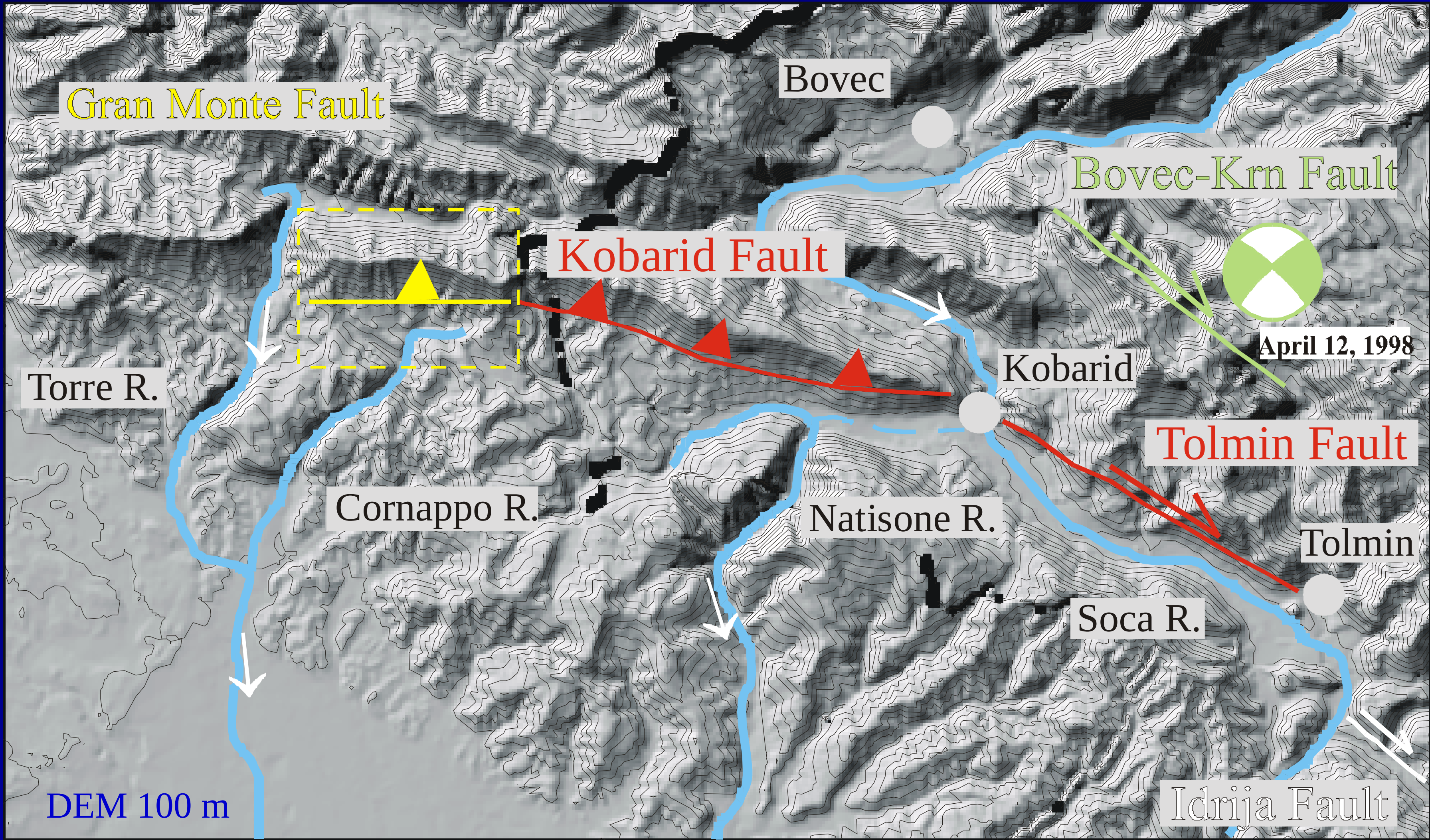

Input Fault Model: L 30 km, W 10.5 km, M 6.6, θ 290°, δ 70°, λ 146°

The Kobarid-Tolmin Fault (1 Hz): Results

Uniform Seismic Moment Distribution

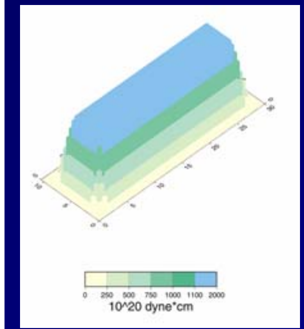

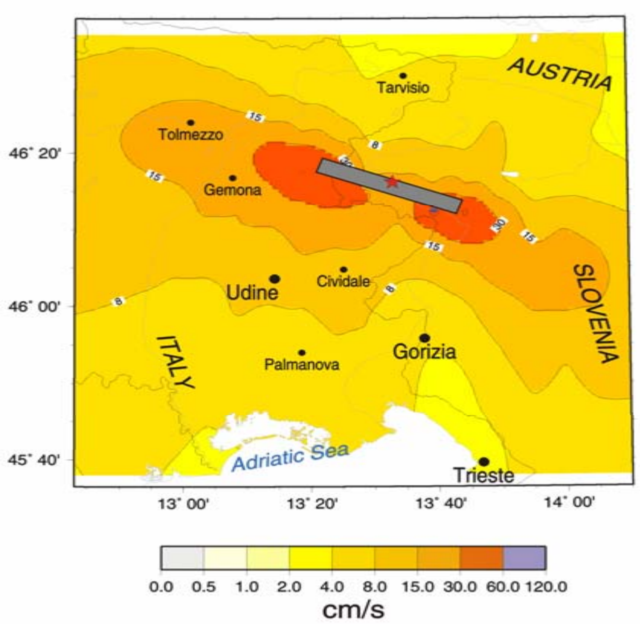

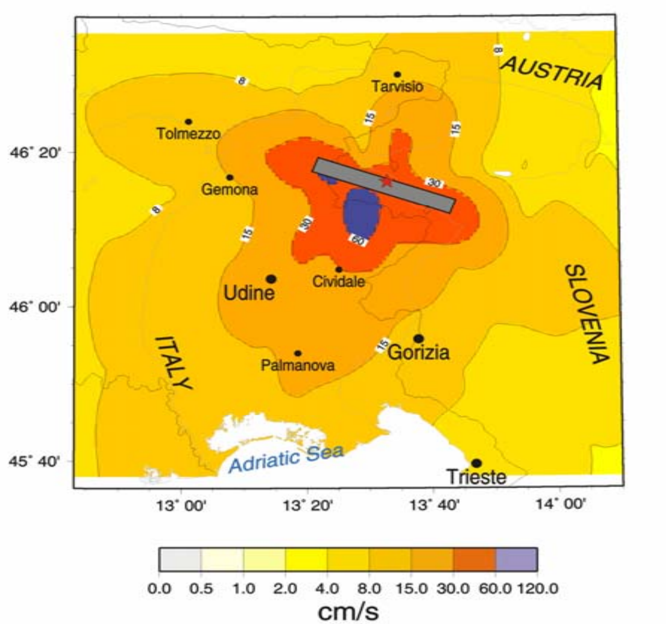

Single Asperity

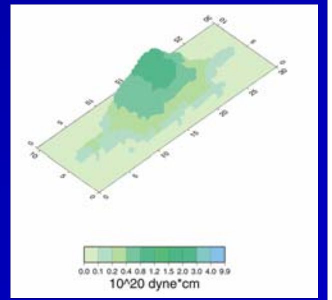

Double Asperity

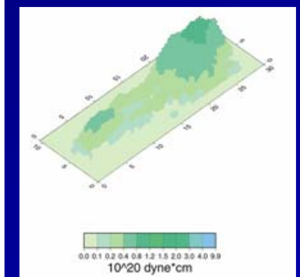

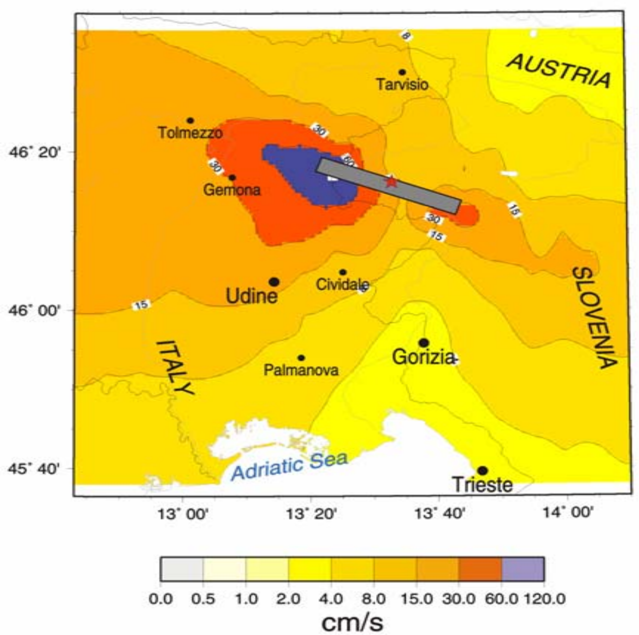

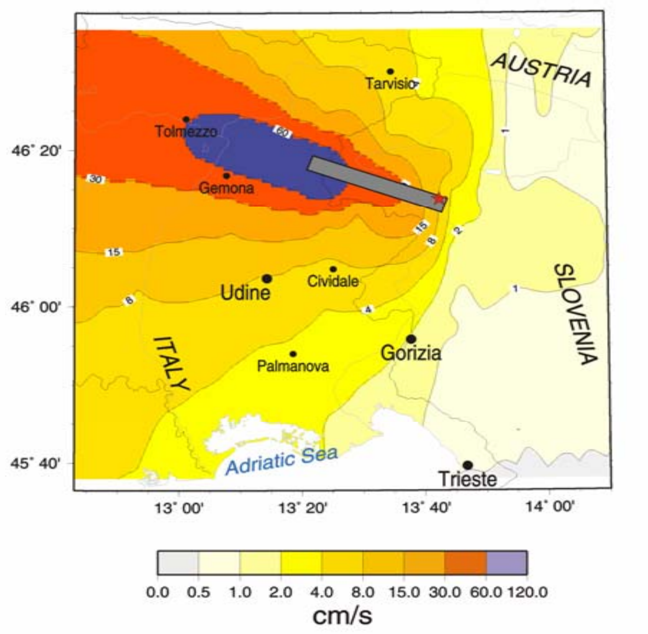

Double Asperity

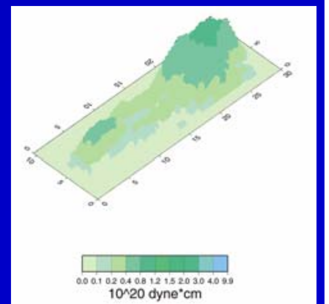

The Tolminka Fault (1 Hz, 2 Hz):

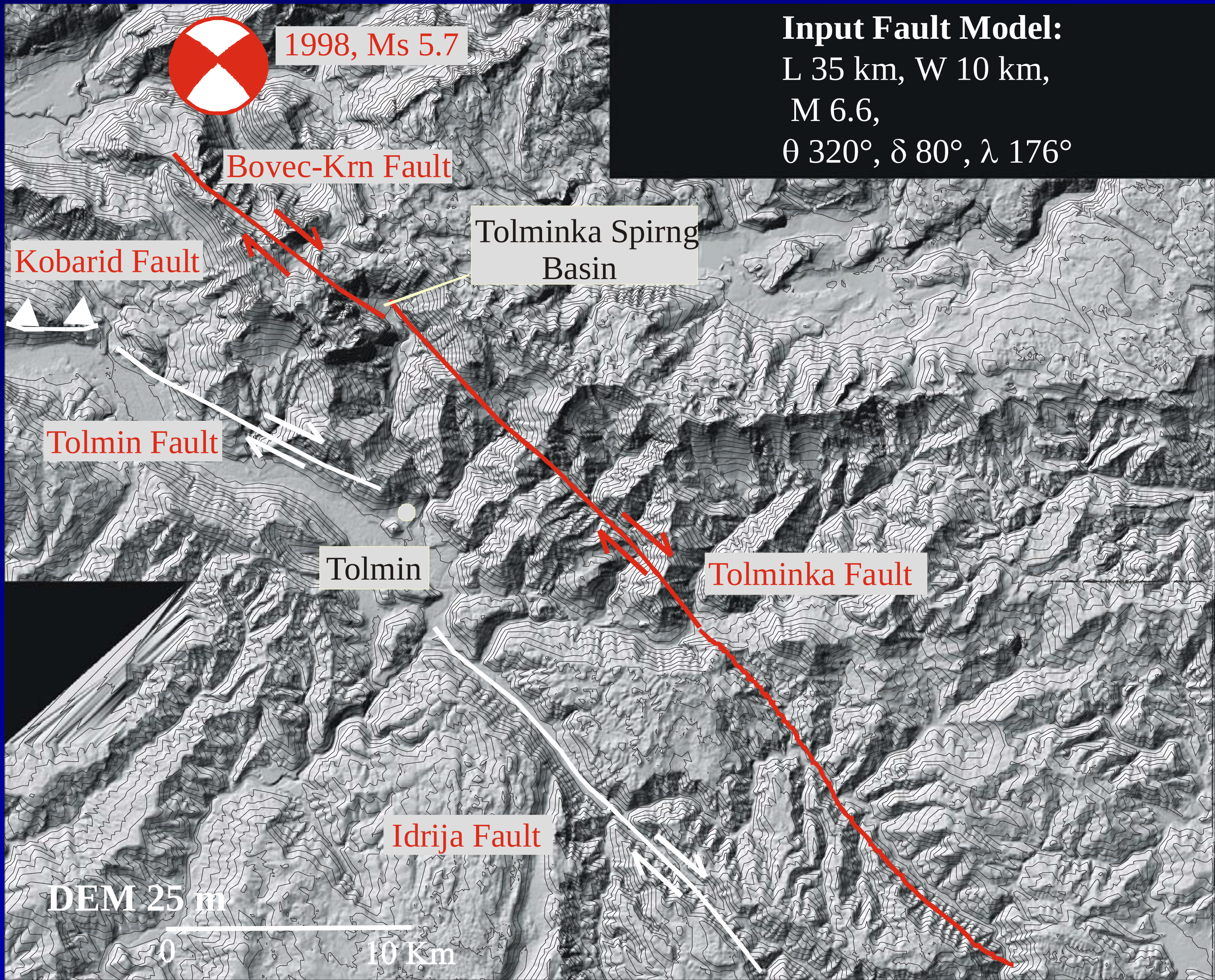

The Tolminka Fault: Results – 1 Hz

Single
Asperity

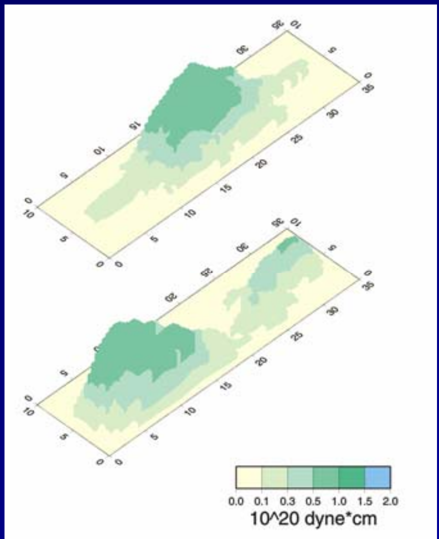

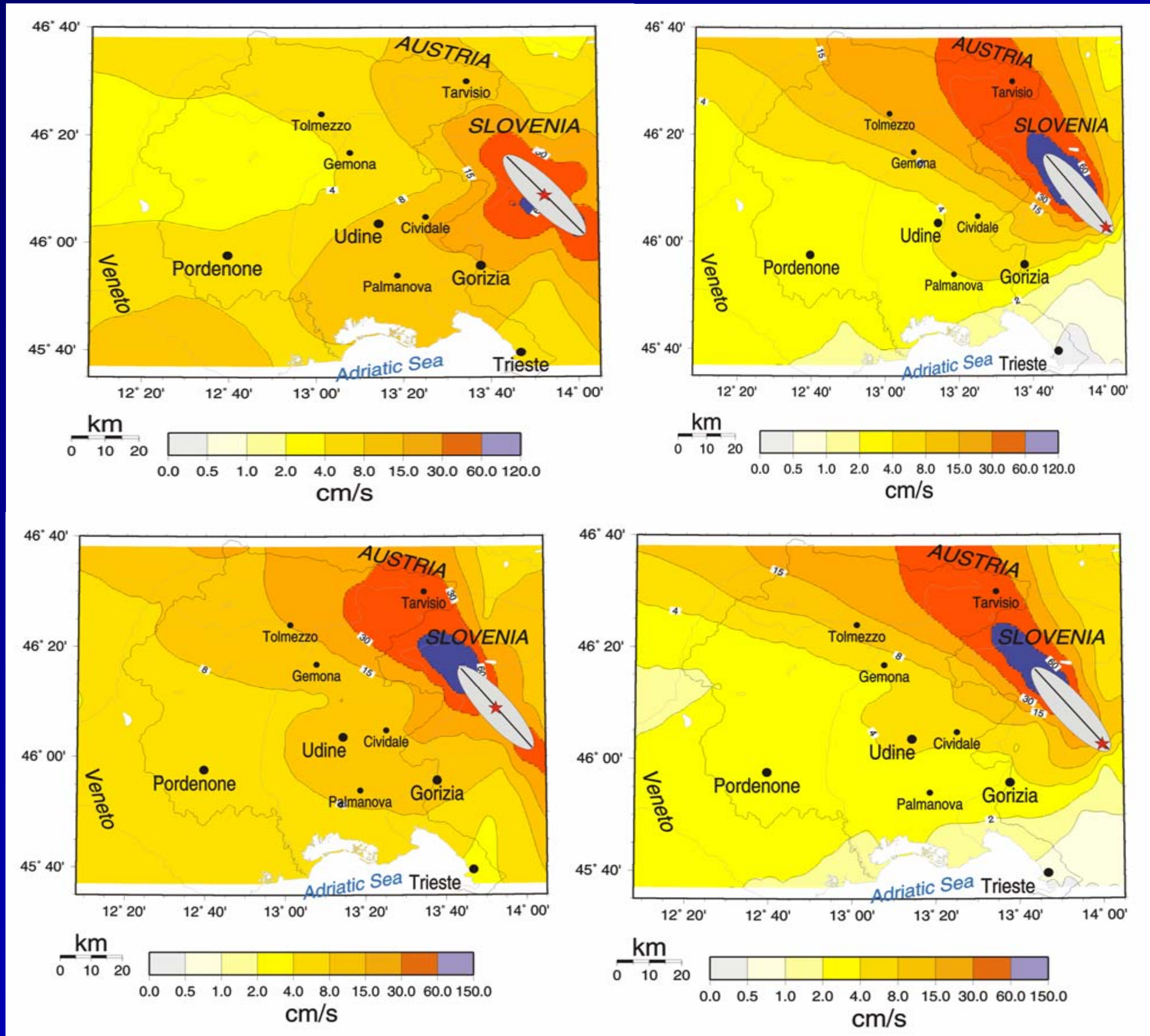

Double
Asperity

Conclusions - 1/3

- The effects of the source directivity and the characteristics of the seismic moment distribution on the fault plane generate a large variability in the seismic hazard values of the analyzed localities. Moreover, the position of the single asperity and the ratio between the two asperities strongly affect the maximum velocity field.

Conclusions - 2/3

- The computed **maximum horizontal velocities** (1 Hz), using 4 active structures at the Alps-Dinarides Junction as input fault models, are **generally larger** than the values predicted by other deterministic seismic hazard studies carried out both in Friuli and in Slovenia using scaled point sources (Panza et al., 2001; Zivcic et al., 2000).

Conclusions - 3/3

- Our **modeling** and estimation of the seismic input at a specific site, when applied to different earthquake scenarios in its surroundings, can be a **powerful**, **economically valid** and **easily applicable** scientific tool for assessing its seismic hazard.

Local waveform inversion for source parameters of a finite fault

Possible pitfalls

The questions we would like to address are:

1. How close is the solution of this (unstable) problem to the correct one?

2. How does poor knowledge of crustal structure in the source region affect the estimate of the rupture front location and speed?

3. Since such inversions are non-unique, what methods can one use to choose the “correct” solution from among the multiplicity of solutions?

Since these questions cannot, in fact, be answered when working with real data, we set up a problem using artificial data

Source model

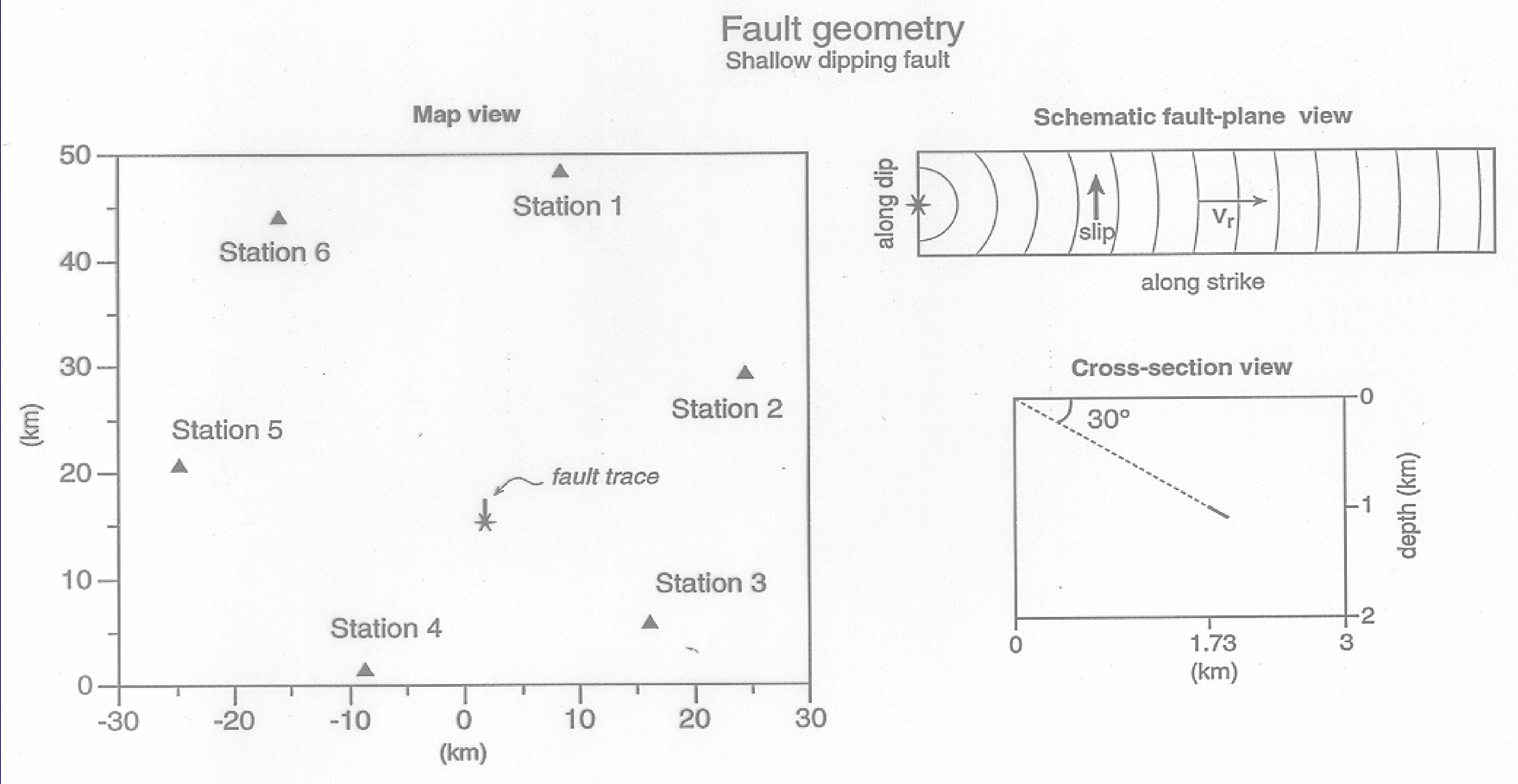

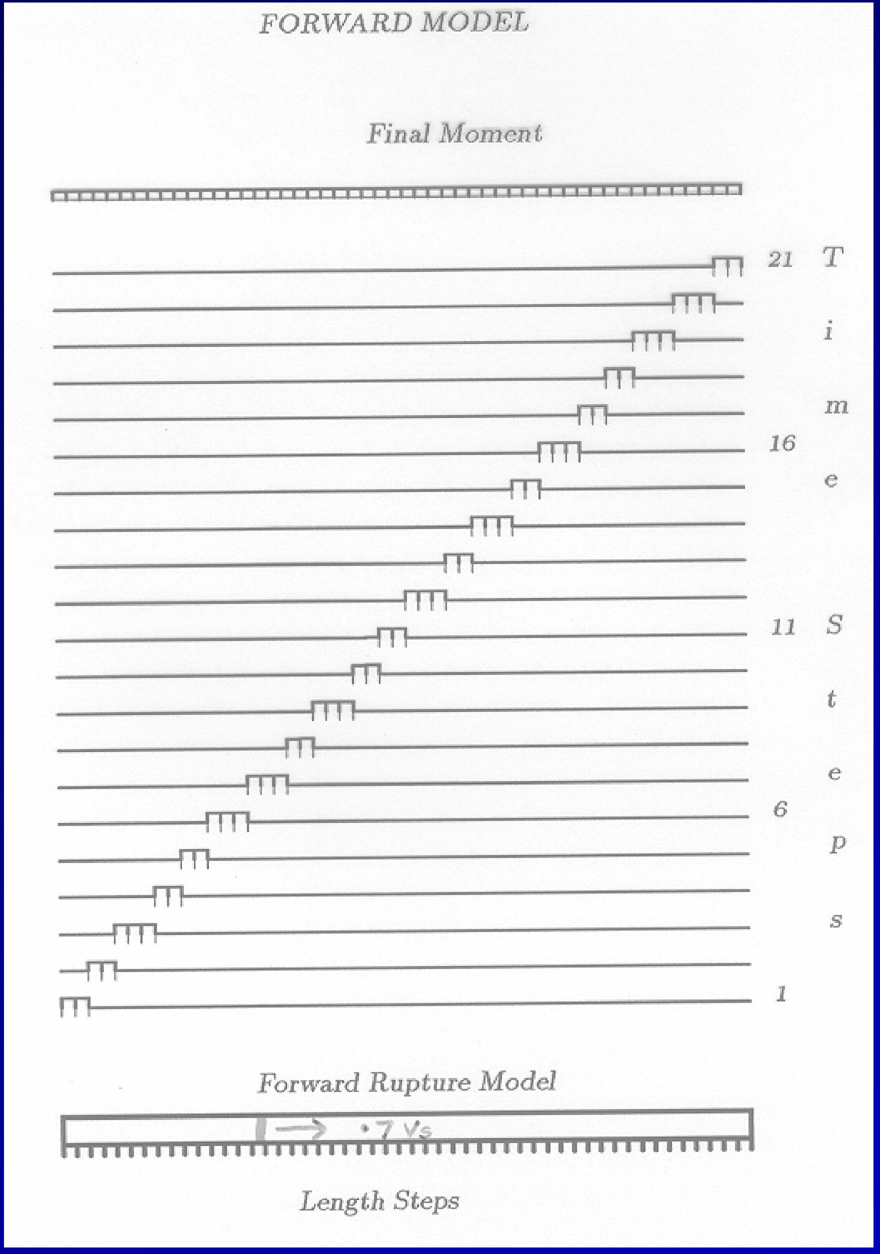

Forward model

1×10^{11} Nm of moment are released at each grid, which is allowed to slip only once

Rupture speed = 0.7 β

In the first set of cases, the inverse problem is solved using the SAME spatial and temporal grid sizes as those used to generate the synthetic (noise-free) data

Inversion methods

First approach:
SVD, minimize L2 norm
Constrain moment value
Remove small eigenvalues
Solution with smallest first differences

Second approach:
Linear programming, minimize L1 norm
Use different physical constraints
Smallest second differences

Case 1a - conclusions

Even if we constrain the rupture front in the inversion to the true front, we are unable to reproduce the final constant moment distribution and the source time function, when we use the SVD method: many small, negative values of moment rates are produced

Case 1b - conclusions

When we constrain the moment rates to be POSITIVE (using the linear programming method) we are able to reproduce the final constant moment distribution and the source time function correctly!

Case 1c - conclusions

When we constrain the rupture front to move faster than the true one and also allow all cells behind it to continue to slip, we are able to reproduce the solution (moment-rate history, final moment, source time function) as long as the POSITIVITY constraint is used

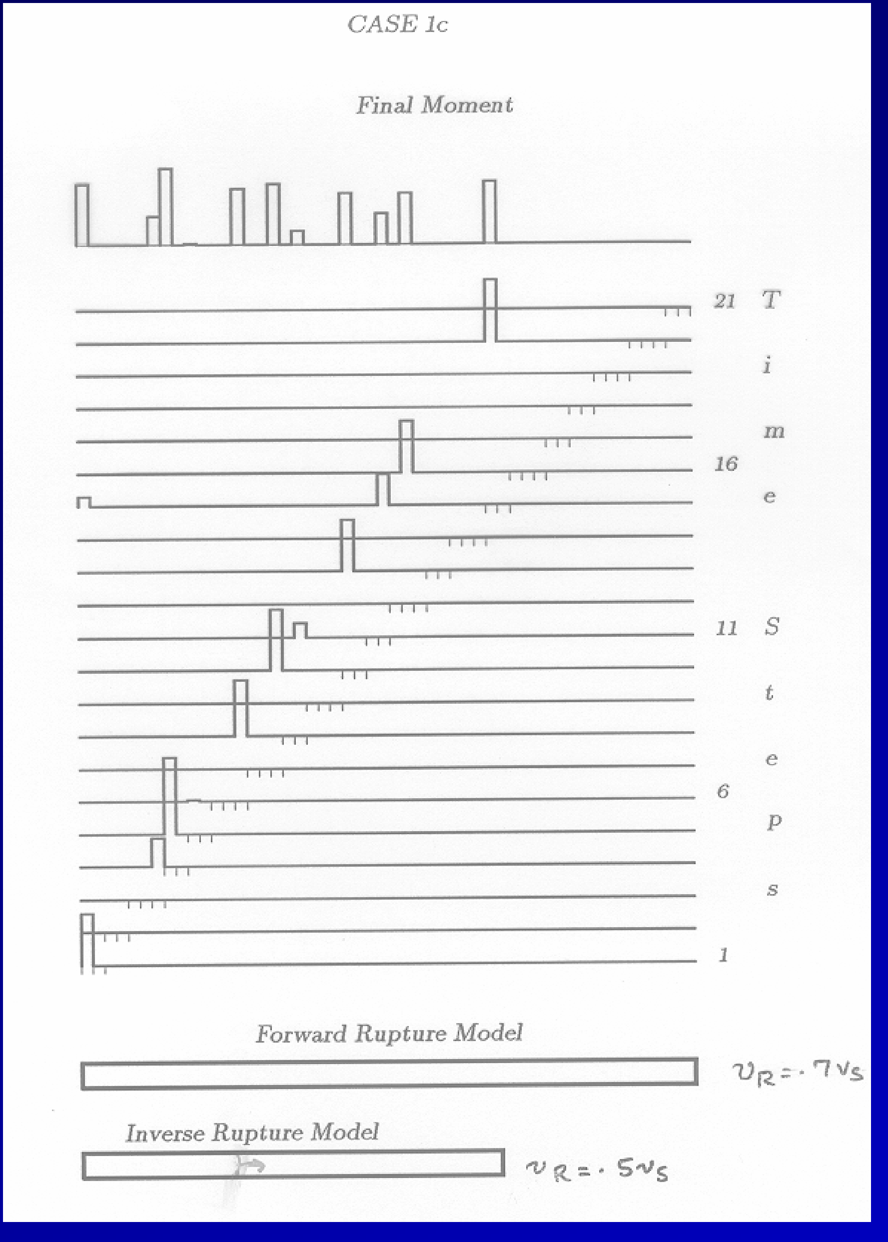

Case 1c
Rupture front

Forward model = 0.7 β
Inverse model = 0.5 β

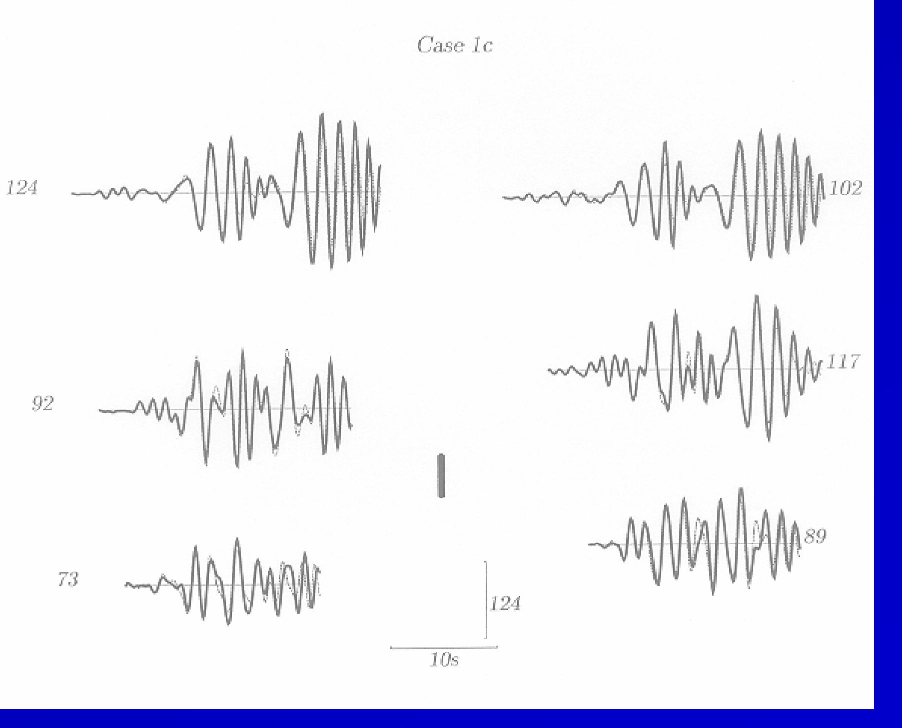

Case 1c - conclusions

If the rupture front is constrained to move more slowly then the true one, we are unable to reproduce any aspect of the solution correctly, even with the positivity constraint. Constraining the seismic moment to the true one does not improve the solution.

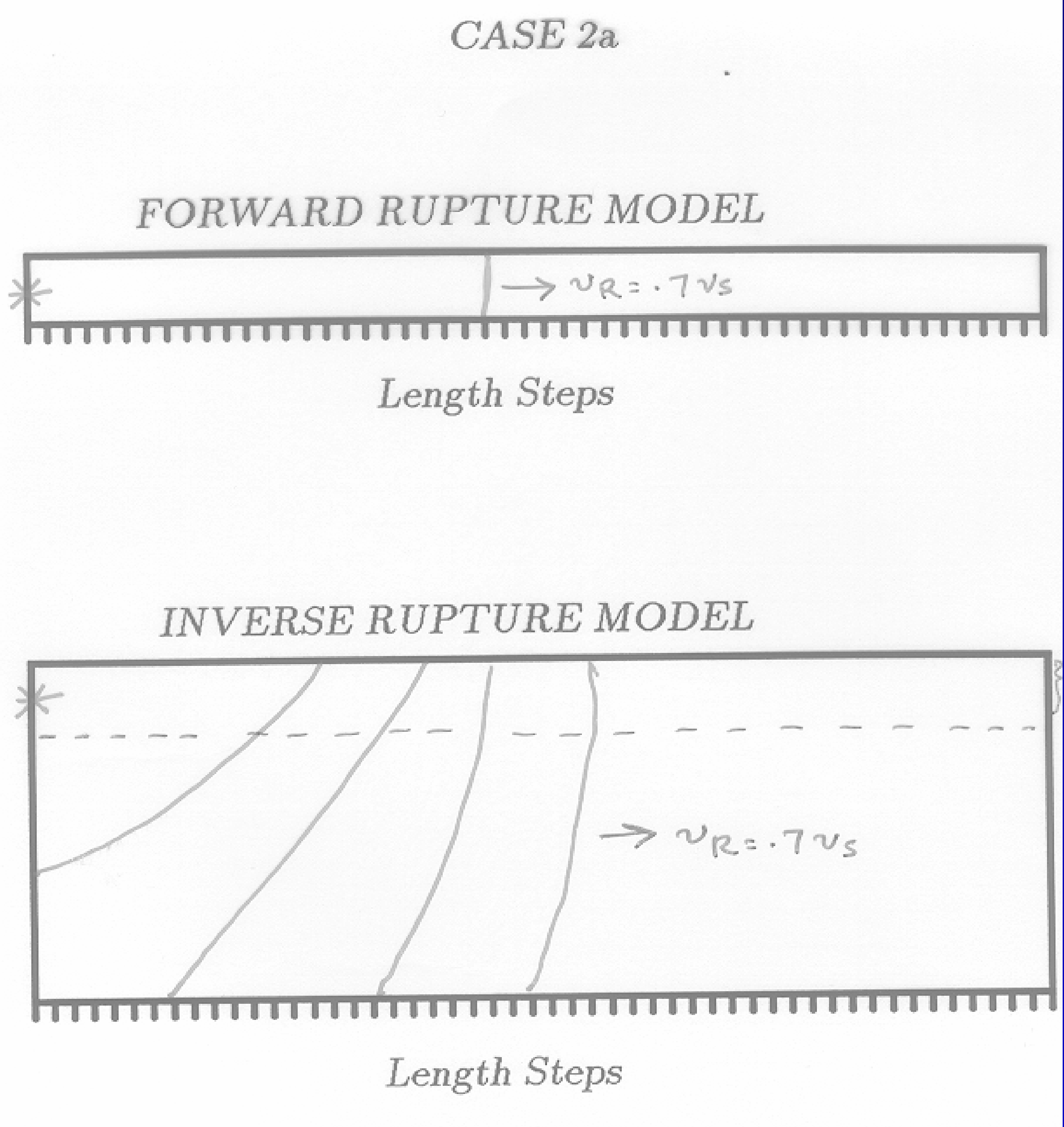

Case 2a

Wider fault

Same rupture speed in forward and inverse model

0.7 β

Case 2a - conclusions

If we use a wider fault and the correct rupture speed and allow cells to release moment only once in the inversion, and also impose the positivity constraint, then the moment is only released at the correct depth in the solution, even though moment release at deeper parts of the fault was permitted

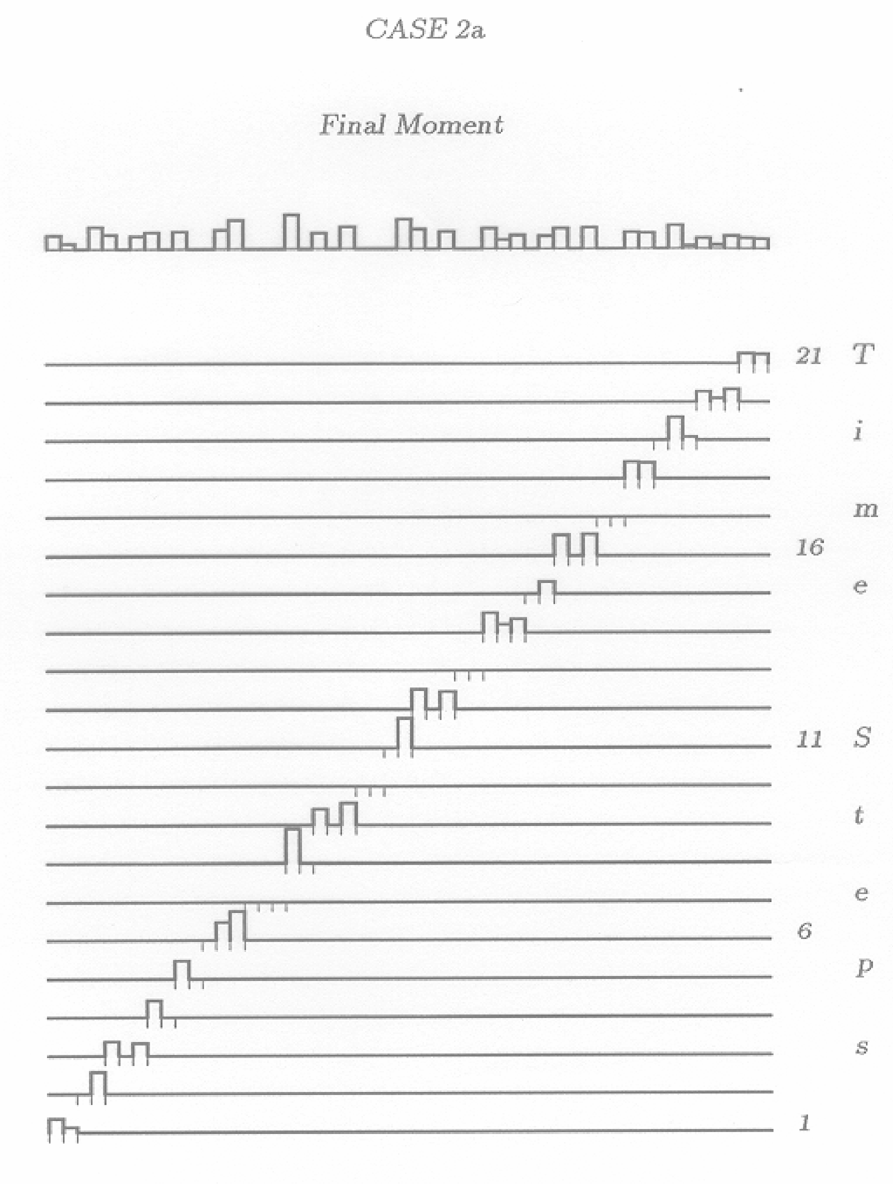

Case 2a Wider fault

Inversion results

The constant moment release is reproduced approximately

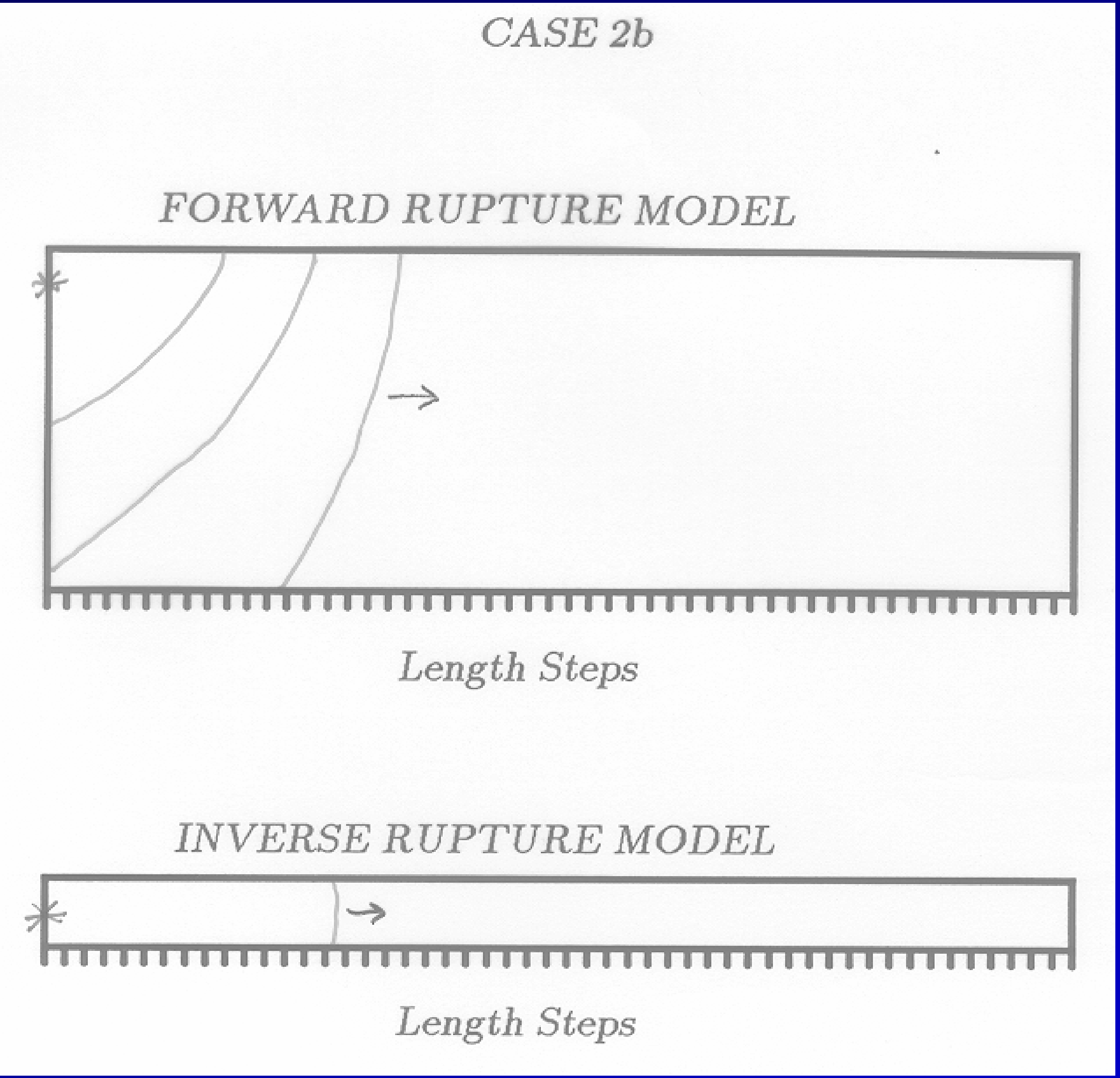

Case 2b
Narrower fault

Same rupture speed
0.7 β

Case 2b - conclusions

If we use a narrower fault than the true one in the inversion, we obtain the correct moment and centroids, but are unable to reproduce the source time function and the uniform moment release at the rupture front

But we are able to fit the data!

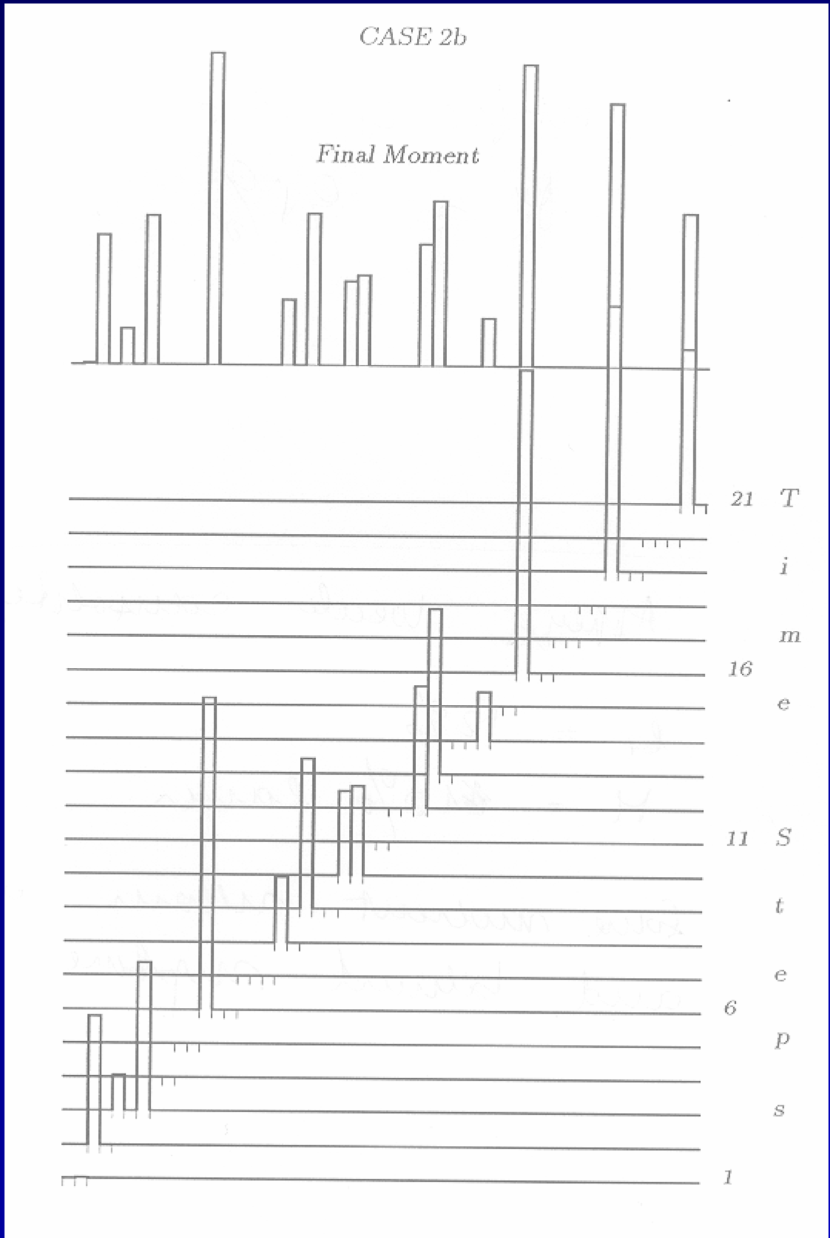

Case 2b
Narrower fault

Strongly non-uniform moment distribution (asperities!)

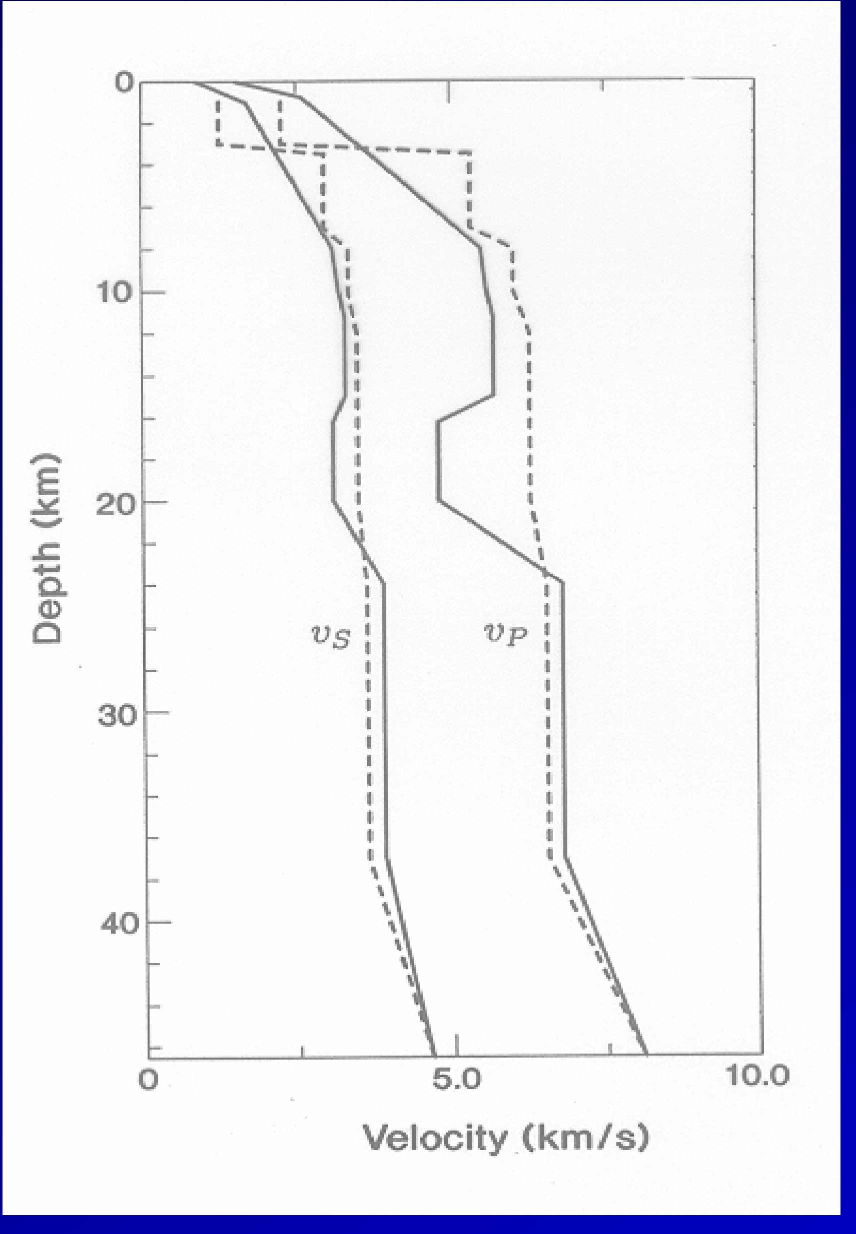

Case 3a

Different medium used

in forward (M1, continuous) and inverse model (M2, dashed)

Case 3a
Different medium

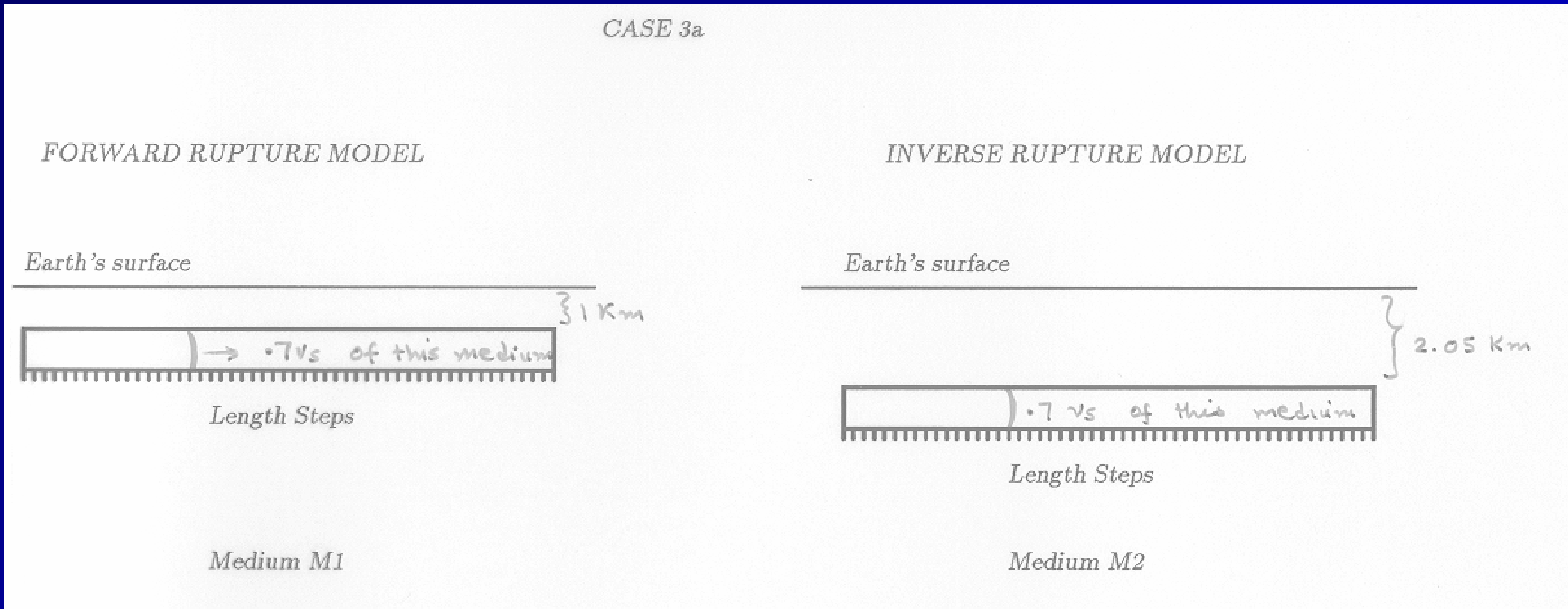

Case 3a - conclusions

Incorrect source structure leads to poor fitting of the data and the solution is not reproduced. Instead, this incorrect source structure is transformed into ARTIFACTS of the solution!

An illustration of the effect of model noise

Case 3a

Incorrect source structure

Appearance of artifacts: a GHOST front Behind the main rupture front

Region excluded by weak causality constraint

CONCLUSIONS

In summary, if the Earth structure is known, then we can determine the rupture front location in time, as long as we use a larger fault area and larger rupture speed than the true ones.

CONCLUSIONS

All our negative conclusions, say the fact that we are unable to reproduce the correct solution without the positivity constraint, will hold for more complex cases

CONCLUSIONS

On the other hand, our positive conclusions, say the cases when we can reproduce the rupture front position correctly by using the positivity constraint, is only applicable to the simple forward model studied here

CONCLUSIONS

This study demonstrates the problems we encounter even for the simple case of a Haskell-type faulting model. Clearly more realistic models, like crack models, and models with larger variability of rupture propagation speeds would present even greater difficulties.

Acknowledgments

- **The presentation is based on the following papers:**

- Aoudia, A., Sarao', A., Bukchin, B. and Suhadolc, P., 2000. The Friuli 1976 event: a reappraisal 23 years later. Geophys. Res. Lett., 27, 4, 573-576.
- Bajc, J., Aoudia, A., Sarao', A., and Suhadolc, P., 2001. The 1998 Bovec-Krn mountain (Slovenia) earthquake sequence. Geophys. Res. Lett., Vol. 28, No. 9 , p. 1839-1842.
- Das, S. and Suhadolc, P., 1996. On the inverse problem for earthquake rupture. The Haskell-type source model. J. Geophys. Res., 101, 5725-5738.
- Fitzko, F., Suhadolc, P. & Costa, G., 2004. Realistic strong ground motion scenarios for seismic hazard assessment studies at the Alps-Dinarides junction. In: Earthquake: Hazard, Risk, and Strong Ground Motion, Y.T.Chen, G.F.Panza and Z.L.Wu (eds.), Seismological Press, Beijing, 361-377.
- Fitzko, F., Suhadolc, P., and Costa, G., Panza, G.F., 2005. The 1511 western Slovenia earthquake: constraints on source mechanism and location from modeling of macroseismic data. Submitted to Tectonophysics.
- **Some parts of the presentation have been produced for the Civil Defence of the Friuli Venezia Giulia Region (Italy)**